2018

Long-term Changes in Extreme Air Pollution Meteorology and Implications for Air Quality

Pei Hou
Michigan Technological University, phou@mtu.edu

LONG-TERM CHANGES IN EXTREME AIR POLLUTION METEOROLOGY AND IMPLICATIONS FOR AIR QUALITY

By

Pei Hou

A DISSERTATION

Submitted in partial fulfillment of the requirements for the degree of

DOCTOR OF PHILOSOPHY

In Atmospheric Sciences

MICHIGAN TECHNOLOGICAL UNIVERSITY

2018

This dissertation has been approved in partial fulfillment of the requirements for the Degree of DOCTOR OF PHILOSOPHY in Atmospheric Sciences.

Department of Geological and Mining Engineering and Sciences

Dissertation Advisor: *Dr. Shiliang Wu*

Committee Member: *Dr. Paul V. Doskey*

Committee Member: *Dr. Jessica J. McCarty*

Committee Member: *Dr. Raymond A. Shaw*

Department Chair: *Dr. John S. Gierke*

Dedication

To my dearest Fan Yang

who is my love, the light of my life.

Contents

List of Figures

List of Tables

Preface

The publications presented in this thesis are parts of the research work conducted at Michigan Technological University from 2013 to 2018. Long-term changes in extreme air pollution meteorological events and their implications for air quality are studied through observational data analysis and a global three-dimensional chemical transport model (GEOS-Chem). Mrs. Hou did all the writings with the help of Dr. Wu and other co-authors.

Chapter 2 presents the analysis of heat waves, temperature inversions, and atmospheric stagnation episodes to study their long-term trends and their relationships with ozone and fine particulate matters. In this chapter, Mrs. Hou conducted the data collection and analysis under the supervision of Dr. Wu.

Chapter 3 presents the construction of logistic regression models to predict high pollution episodes with the occurrences of extreme air pollution meteorology. Mrs. Hou conducted the development and the validation of models after finishing the related data analysis under the supervision of Dr. Wu.

Chapter 4 presents the perturbation tests that examine the sensitivities of black carbon lifetimes to different precipitation characteristics. Mrs. Hou conducted the simulations and the data analysis under the supervision of Dr. Wu and Dr. McCarty.

Acknowledgments

I would like to thank my advisor Dr. Shiliang Wu for his patient and inspiring advice. I am really grateful for all of his guidance, encouragement, and valuable suggestions. My sincere thank goes to all my committee members, Dr. Paul Doskey, Dr. Jessica McCarty and Dr. Raymond Shaw, for their help and time. I would thank all the members of my research group: Dr. Yaoxian Huang, Aditya KumarXueling Li, Mackenzie Roeser, Dr. Ka Ming Wai, and Dr. Huanxin Zhang. I also want to thank Dr. Will Cantrell, Dr. Hongyu Liu, and Dr. Bo Zhang for fruitful discussions.

Thank U.S. EPA (Grant 83518901), Earth, Planetary, and Space Sciences Institute (EPSSI), Atmospheric Sciences program, and the Department of Geological and Mining Engineering and Sciences for their support. Thank Michigan Technological University for the peaceful study environments and all the excellent courses.

I thank all the people who have contributed to the datasets we applied in the dissertation. The NCEP reanalysis data and NCEP-DOE AMIP-II reanalysis data were provided by NOAA/OAR/ESRL PSD, Boulder, Colorado, USA, and were accessed through their Web site at http://www.esrl.noaa.gov/psd/. The MERRA data used in this study were provided by the Global Modeling and Assimilation Office (GMAO) at the NASA Goddard Space Flight Center through the NASA GES DISC online

archive. And TRMM, GCAP2, and AQS data ware provided by NASA, Harvard, and U.S. EPA, respectively. Superior, a high-performance computing infrastructure at Michigan Technological University, was used in obtaining results presented in this publication.

And I want to thank my friends and family. Many thanks go to Weilue He for his pieces of advice on the academic part and lots of help in my life. Thank for companies, encouragements, and concerns from Yihe Wang and Zhipei Chen. I would like to thank my family. I appreciate my parents for teaching me valuable life lessons and having confidence in me. Last but not the least, I want to thank my husband Fan Yang who gives me lots of support and love. He not only makes my life happier but also makes me a better person.

Abstract

Extreme air pollution meteorology, such as heat waves, temperature inversions, and atmospheric stagnation episodes, can significantly affect air quality. In this study, we analyze their long-term trends and the potential impacts on air quality. The significant increasing trends for the occurrences of extreme meteorological events in 1951-2010 are identified with the reanalysis data, especially over the continental regions. A statistical analysis combining air quality data and meteorological data indicates strong sensitivities of air quality, including both average air pollutant concentrations and high pollution episodes, to extreme meteorological events. Results also show significant seasonal and spatial variations in the sensitivity of air quality to extreme air pollution meteorology.

Based on the sensitivity studies of air quality to air pollution meteorology, statistical models are constructed to predict the likelihood of extreme air pollution episodes with the status of extreme air pollution meteorology in two consecutive days. Our statistical models present reasonable estimation of air pollution days validated with observations. Our method is more computational efficiency and user-friendly than the complicated atmospheric chemistry models. It could be a useful tool for air quality forecast, in particular for projecting the risk of extreme air pollution episodes.

Extreme meteorological events related to precipitation, such as drought or heavy precipitation, are also important for air quality. To get a better understanding of the relationship between precipitation features and air quality, we examine the sensitivities of air pollutants to the changes of various precipitation characteristics in the context of climate change. Perturbation studies are tested with GEOS-Chem model to isolate the roles of precipitation frequency, precipitation intensity, and total precipitation amount in the lifetime of black carbon (BC). We find that the atmospheric lifetimes of BC are more sensitive to precipitation frequency than precipitation intensity. The relationship between the lifetime of aerosols and the change of precipitation characteristics offer a simple tool to examine the effects of long-term changes of precipitation characteristics on atmospheric aerosols in various regions.

Chapter 1

Introduction

It has been known that air pollution risks human health, and people have taken a lot of efforts to understand the causes and the impacts of air pollution. Ozone and fine particulate matters ($PM_{2.5}$) are the two most general and harmful air pollutants in the atmospheric boundary layer that threat the public health and damage the environment [*Englert*, 2004; *McKee*, 1993]. The increasing trend of air pollution due to human activity has been found locally and globally. Results showed that the levels of ozone concentrations have increased by approximately two times when compared the current levels with those were measured over a century ago [*Vingarzan*, 2004]. Conditions might be even worse in some local areas. For example, it was found that surface ozone concentration increased by a factor of 2.2 during 1989-1991 at Arosa in Switzerland [*Staehelin et al.*, 1994]. With the efforts of controlling air pollution by reducing anthropogenic emissions, air quality improved in most developed countries and some developing countries. Taking China as an example, the $PM_{2.5}$ levels retrieved from the satellite showed an increasing trend between 2004 and 2007 followed by a decreasing trend between 2008 and 2013 [*Ma et al.*, 2016]. Although the situations are getting better, the issues of ozone and $PM_{2.5}$ are still our current and future challenges. Previous studies revealed that even low concentrations of ozone and $PM_{2.5}$ have a relationship with mortality [*Brunekreef and Holgate*, 2002; *Council et al.*, 2008; *Schwartz et al.*, 2002]. Therefore, although current air quality standards are helpful to reduce morbidity and mortality related to air pollution, stricter environment management is needed to further control the air pollution with the purpose

of improving public health.

Meteorology is one of the most important factors that impact air quality. Several processes related to air quality can be affected by meteorology, including emissions, chemical reactions, dry and wet deposition, and transport [*Kinney*, 2008]. Some of the meteorological events occur occasionally but have a strong influence on air quality. These rare but important events are taken as extreme air pollution meteorological events in this study. It was found that climate change may increase the occurrence of extreme meteorological events, and thus moderate our efforts in decreasing air pollution [*Jacob and Winner*, 2009]. Therefore, the effects of reducing anthropogenic emissions with the purpose of protecting public health might be canceled off by climate change [*Leibensperger et al.*, 2008]. This offset is taken as climate change penalty, which complicates the management of environment [*Wu et al.*, 2008]. There have been many studies about the potential effects of climate change on air quality [*Alexander and Mickley*, 2015; *Dawson et al.*, 2014; *Dentener et al.*, 2006; *Doherty et al.*, 2013; *Fiore et al.*, 2012, 2015; *Gao et al.*, 2013; *Lei et al.*, 2012; *Pfister et al.*, 2014; *Pye et al.*, 2009; *Rieder et al.*, 2013, 2015; *Weaver et al.*, 2009; *Wu et al.*, 2008]. Most of these analyses have focused on the impacts of meteorological variables, such as temperature, humidity, wind speed, and precipitation, on air quality under normal meteorological conditions. It has been shown that extreme air pollution meteorological events have stronger correlations with high pollution episodes[*Camalier et al.*, 2007; *Jones et al.*, 2010; *Thompson et al.*, 2001]. Therefore, more attention

should be paid. In this dissertation, we will mainly focus on five types of extreme air pollution meteorological events, including heat waves, temperature inversions, atmospheric stagnation episodes, fires, and extreme precipitation events. In the following paragraphs, we will give a brief introduction about each type of extreme air pollution meteorological events and previous studies about their impacts on air quality.

Heat waves, which are the persistent high surface temperature at a local region, show a serious threat to human health. A large number of heat-related deaths were found in heat waves, especially in a series of record-breaking events: more than 700 heat-related deaths were found in the Chicago heat wave event in 1995, and the number exceeded 70,000 in the long-lasting heat wave event happened in Europe in 2003 [*Robine et al.*, 2008; *Semenza et al.*, 1996]. The heat-related death is related to the respiratory and cardiovascular diseases that especially harmful to elders [*Poumadere et al.*, 2005]. The morbidity and mortality in 2003 Europe event draw much attention to the study of heat waves. The previous study about the air quality during heat waves pointed out that elevated air pollution is another factor that led to death besides the effect of high temperature itself [*Shaposhnikov et al.*, 2014]. The extreme high temperature in heat waves is the direct reason for the high air pollution. Other meteorological features associated with the accompanied high-pressure system, such as low wind speed and clear sky, are the indirect causes of the enhanced air pollution.

Both observations and simulations have indicated that higher temperature elevates

ozone [*Cardelino and Chameides*, 1990; *Dawson et al.*, 2007b; *Rasmussen et al.*, 2012]. *Fiore et al.* [2003] found that the concentrations of ozone increased with the temperature non-linearly in summertime in California, although the ozone formation depressed in the extreme high temperature. The strong correlation between higher temperature and higher ozone concentrations related to multiple factors of the tropospheric ozone formation. Reactions 1.1-1.3 show the typical mechanism of ozone production in a polluted atmosphere [*Jacob*, 1999].

$$RH \ + \ OH \ \xrightarrow{O_2} \ RO_2 \ + \ H_2O \tag{1.1}$$

$$RO_2 \ + \ NO \ \rightarrow RO \ + \ NO_2 \tag{1.2}$$

$$NO_2 \ + h\nu \ \xrightarrow{O_2} \ NO + O_3 \tag{1.3}$$

where nitrogen oxides ($NO_x \ = \ NO \ + \ NO_2$) and hydrocarbon (RH) are two primary precursors of ozone formation.

When surface temperature increases, the emissions of these precursors can be boosted by the increase of 1) isoprene, monoterpenes, carbon monoxide, and other carbon-related emissions released by vegetations; 2) the decomposition of peroxyacetylnitrate (PAN) in higher temperature resulting an increase of both NO_x and HO_x; 3) evaporation rate resulting in more hydrocarbons (RH) in the atmosphere; 4) the emission from wildfire due to higher probability of wildfire; 5) anthropogenic emission due to

the potential usage of electrical cooling system in extreme hot days. The enhancement of chemical reaction rate in the higher temperature may further increase the concentration of ozone in heat waves in a polluted atmosphere. What's more, the stomata of vegetations closed in extreme high temperature to protect the vegetation from temperature stress and water stress [*Emberson et al.*, 2000]. With inactive stomata, the dry deposition decreases that increases the lifetime of air pollutants.

Except for temperature, other meteorological factors associated with heat waves are also important to the elevated ozone concentration. For example, heat waves are usually accompanied by the high-pressure system and the clear sky, which would increase the downward shortwave radiation, and therefore increase the photolysis rate of NO_2. In addition, the low surface wind speed associated with heat waves reduce the transport, which would enhance the accumulation of air pollutants in a local region. The low relative humidity also favors the increase of ozone, since the reaction with water is one of the removal paths of ozone [*Singla et al.*, 2011].

Heat waves also affect the concentrations of $PM_{2.5}$. The relationship between $PM_{2.5}$ and heat waves are complicated because the responses of $PM_{2.5}$ to heat waves depend on their chemical compositions. High temperature and the associated clear sky would enhance the oxidation and photochemical process of aerosols, resulting in the increase of components like sulfate and the decrease of components like nitrate. Higher concentrations of fine particulate matters were found when heat waves happened [*D'Ippoliti*

et al., 2010; *Theoharatos et al.*, 2010]. Since wet deposition is the main sink to remove aerosols, especially fine particulate matters, less precipitation in sunny days leads to the increases in the lifetime of aerosols. The concentrations of $PM_{2.5}$ would also be boosted by more occurrences of wildfires in the hot and dry environments [*McKenzie et al.*, 2004; *Westerling et al.*, 2006].

The temperature inversion is a type of extreme air pollution meteorology with the temperature increasing with height. Temperature usually decreases with the increase of altitude in the troposphere. When the air above is colder than the surface, especially when the adiabatic lapse rate is smaller than environmental lapse rate, air pollution at surface easily got transported to higher altitude through convection. When the temperature inversions happen, vertical air motion is strongly suppressed in the inversion layer. Because temperature inversions significantly suppress the convection, it is expected that the occurrences of temperature inversions enhance the local air pollution. The accumulation of air pollutants would become even worse if there are some emission sources within the inversion layers.

Researches found that a large number of air quality episodes in spring and winter were related to inversion and stable stratification [*Janhäll et al.*, 2006; *Kukkonen et al.*, 2005; *Schnell et al.*, 2009; *Wallace et al.*, 2010]. For example, the occurrences of temperature inversions coincided with the highest ozone and PM concentrations in London smog event in 1952 [*Laskin*, 2006]. It has been found that temperature

inversion can explain some high surface smoke concentrations, though a strong horizontal wind may help to transport air pollutants and thus weaken the blocking effect of inversion [*Milionis and Davies*, 1994]. In contrast, weak wind or special topography (like valleys) will limit the horizontal transport of air mass and thus increase the cumulative effect of temperature inversion.

Atmospheric stagnation episodes occur when air parcels stay in one region for a long period of time. Atmospheric stagnation is defined by the low wind speed and the lack of precipitation when local pollution tends to have less horizontal transport and less wet deposition. In atmospheric stagnation episodes, the pollutants from local emission accumulate over time, which cause higher risks of health problems for people living in those areas. Situations become worse when both temperature inversion and atmospheric stagnation happen at the same time. Although some studies have shown a positive correlation between pollutants and atmosphere stagnation, especially in several high air pollution events, the correlations are distinct under different conditions [*Leung and Gustafson*, 2005; *Logan*, 1989]. Similar to temperature inversions, the relationship between atmospheric stagnation episodes and air pollutants is affected by the source of emissions. When the main emission source is out of the stagnation region, the air pollution may decrease in atmospheric stagnation episodes by blocking the polluted air parcels out of the region.

With climate change, the occurrences of wildfires may increase due to the changes of

several factors, such as temperature, humidity, and lightning [*Hantson et al.*, 2016; *Stavros et al.*, 2014]. The fire emissions are important for the air quality. Wildfire emission is a large natural source of various types of aerosols that fires even have strong impacts on the global burden of fine particulate matters [*Voulgarakis et al.*, 2015]. Fires also increase the production of ozone by emitting NO_x, CO, and non-methane volatile organic compounds (NMVOC) [*Voulgarakis and Field*, 2015].

Extreme precipitation events, such as drought and flood, also affect air quality [*Rosenfeld et al.*, 2008]. Drought occurs with a prolonged period of extremely low surface precipitation, which is unfavorable for the removal of pollutants. Moreover, drought might be exacerbated by heat waves and atmospheric stagnation episodes that degrade air quality. These extreme precipitation events mainly affect wet deposition, which is a major removal process for aerosols and soluble gases in the atmosphere [*Atlas and Giam*, 1988; *Radke et al.*, 1980]. There are mainly two types of wet scavenging: rainout (in-cloud scavenging) and washout (below-cloud scavenging). Rainout is responsible for the cloud droplet activation process in a supersaturated environment above cloud base where aerosol particles serve as cloud condensation nuclei or ice nuclei, while washout is the collection of aerosol particles by hydrometeors below cloud base.

Most previous studies focused on the correlation between air pollution and total precipitation amount or precipitation intensity [*Cape et al.*, 2012; *Pye et al.*, 2009; *Tai*

et al., 2012]. For example, *Dawson et al.* [2007a] found a strong negative correlation between precipitation intensity and $PM_{2.5}$ concentrations over a large domain of eastern US. Only a few previous studies considered the precipitation frequency. *Jacob and Winner* [2009] claimed that the precipitation frequency dominates the wet deposition compared with precipitation intensity because the wet scavenging due to precipitation is very efficient. *Fang et al.* [2011] projected that wet deposition has a stronger spatial correlation with precipitation frequency than intensity over US region in January, although they concluded that frequency is a minor factor to affect the wet deposition in the context of climate change.

A warmer climate can change the occurrence of extreme air pollution meteorological events discussed above, and thus affect air quality [*Leung and Gustafson*, 2005]. *Meehl and Tebaldi* [2004] claimed that heat waves would become more intense, more frequent, and longer-lasting in the second half of 21st century. This suggests that air pollution related to heat waves might become more severe in the future. *Horton et al.* [2014] also predicted that there would be more atmospheric stagnation events in the future climate, and stagnation episodes will last longer. This will enhance the accumulation of pollutants around the surface and thus increase the risk of public health. Global climate change also implies significant perturbations of precipitation, which can directly affect the wet scavenging process. *Trenberth et al.* [2007] reported that the total precipitation amount increased over land north of 30°N in the past century, but decreased in the tropical region after the 1970s. *Trenberth* [2011] also pointed

out that a warmer climate could lead to less frequent but more intense precipitation, which implies the increase of both floods and droughts. The increase of precipitation intensity and the decrease of precipitation frequency have the opposite effect on air pollution, so the net effect is still unclear.

In Chapter 2, I examine the extreme air pollution meteorological events (heat waves, temperature inversions, and atmospheric stagnation episodes) by studying the long-term evolutions during 1951−2010 and their potential impacts on ozone and fine particulate matter. In Chapter 3, I construct logistic regression models to predict the upcoming high pollution episodes with the occurrences of extreme air pollution meteorological events in two consecutive days. In Chapter 4, I study the extreme precipitation events by making perturbation tests with a model to quantify the effects of precipitation frequency, precipitation intensity, and total precipitation amount on the lifetimes of black carbon.

Chapter 2

Long-term Changes in Extreme Air Pollution Meteorology and the Implications for Air Quality

Reprinted with permission from: Hou, P., and S. Wu (2016), Long-term changes in extreme air pollution meteorology and the implications for air quality, *Scientific Reports*, 6:23792.

2.1 Abstract

Extreme air pollution meteorological events, such as heat waves, temperature inversions and atmospheric stagnation episodes, can significantly affect air quality. Based on observational data, we have analyzed the long-term evolution of extreme air pollution meteorology on the global scale and their potential impacts on air quality, especially the high pollution episodes. We have identified significant increasing trends for the occurrences of extreme air pollution meteorological events in the past six decades, especially over the continental regions. The statistical analysis combining air quality data and meteorological data further indicates strong sensitivities of air quality (including both average concentrations of air pollutants and high pollution episodes) to extreme meteorological events. For example, we find that in the United States the probability of severe ozone pollution when there are heat waves could be up to seven times of the average probability during summertime, while temperature inversions in wintertime could enhance the probability of severe particulate matter pollution by more than a factor of two. We have also identified significant seasonal and spatial variations in the sensitivity of air quality to extreme air pollution meteorology.

2.2 Introduction

Besides affecting the mean values of various meteorological variables, a critical implication of climate change is to alter the frequency and intensity of a suite of extreme meteorological events [*Alexander et al.*, 2006; *Easterling et al.*, 2000; *Francis and Vavrus*, 2012; *Horton et al.*, 2014; *Trenberth et al.*, 2007; *CCSP*, 2008; *Murray and Ebi*, 2012]. Some of these extreme events such as heat waves, temperature inversions and atmospheric stagnation episodes have important implications for atmospheric chemistry and air quality [*Fiala et al.*, 2003; *Filleul et al.*, 2006; *Leibensperger et al.*, 2008; *Ordóñez et al.*, 2010; **?**; *Steiner et al.*, 2010]. There have been many studies on the potential impacts of climate change on air quality [*Alexander and Mickley*, 2015; *Bloomer et al.*, 2009; *Dawson et al.*, 2014; *Dentener et al.*, 2006; *Doherty et al.*, 2013; *Fiore et al.*, 2012, 2015; *Gao et al.*, 2013; *Jacob and Winner*, 2009; *Lei et al.*, 2012; *Pfister et al.*, 2014; *Pye et al.*, 2009; *Rieder et al.*, 2013, 2015; *Tai et al.*, 2012; *Weaver et al.*, 2009; *Wu et al.*, 2008], but most of those analyses have generally focused on the impacts associated with the changes in the average meteorological conditions (such as temperature, humidity, precipitation, etc.). The long-term evolution of extreme air pollution meteorology on the global scale and the potential impacts on air quality have not been thoroughly investigated.

2.3 Method

We examine the evolution of extreme air pollution meteorology in the past six decades based on the National Centers for Environmental Prediction (NCEP) reanalysis dataset [*Kalnay et al.*, 1996]. The dataset covers the 1951-2010 period with a horizontal resolution of 2.5° latitude by 2.5° longitude and a temporal resolution of 6 hours (http://www.esrl.noaa.gov/psd/). To identify the long-term changes in extreme air pollution meteorology (heat waves, temperature inversions and atmospheric stagnation episodes), we compare the climatological data for extreme events for two 30-yr periods: 1951-1980 vs. 1981-2010. We also conduct further analyses to examine the sensitivity of our results to the metrics for definition/identifying air pollution meteorological events and datasets used. To quantify the impacts of extreme air pollution meteorology on air quality, we analyze air quality data (focusing on ozone and $PM_{2.5}$) from the U.S. Environmental Protection Agency (EPA) AQS (http://www.epa.gov/airdata/) database for 2001-2010 together with the meteorology data for the same period. The air quality data are processed into the same spatial resolution as the meteorology data ($2.5° \times 2.5°$) by averaging the available data from all the sites within the same grid cell. Daily average concentrations of $PM_{2.5}$ and afternoon (1-4pm local time) concentrations of ozone (derived from hourly ozone data) are used in the analysis.

For each grid cell, we classify the air quality data into various groups based on the meteorological conditions at the same time (e.g., heat wave group vs. no heat wave group). If any group contains less than three valid air quality data, we exclude that cell from the corresponding analysis. We compare the average concentrations in event group and the no-event group by calculating the percentage changes of concentration (PC) between them (Equation 2.1).

$$PC = \frac{\text{[Event group]} - \text{[No-event group]}}{\text{[No-event group]}} \times 100\% \tag{2.1}$$

To compare the relative importance of various extreme air pollution meteorological events in leading to high pollution episodes for various regions, we carry out further analysis focusing on the high pollution days, which are defined as the top 10% most polluted days for that season during the 2001-2010 period at that location. For days with a specific meteorological event (heat waves, temperature inversions, or stagnation episodes) occurring, we calculate the probability of those days falling in the top 10% high pollution days (i.e. having the top 10% highest concentrations for a given pollutant ozone or $PM_{2.5}$ in this case). This probability (P_{event}) is then compared with the average probability ($\bar{P}$) for all days during the same season (whether or not it has any extreme meteorological event) falling into the top 10% high pollution days ($\bar{P}$ should be equal to 10% following the definition). We also define an impact factor

(I) for a specific meteorological event as

$$I = \frac{P_{event} - \bar{P}}{\bar{P}} \tag{2.2}$$

where

$$\bar{P} = \frac{\text{\# of days with high pollution}}{\text{\# of total days in a given period}} = 10\% \tag{2.3}$$

$$P_{event} = \frac{\text{\# of days with both high pollution and extreme meteorological event}}{\text{\# of days with extreme meteorological event}} \tag{2.4}$$

We use the impact factor to quantify the impacts of extreme air pollution meteorology on high pollution episodes. It clearly shows the changes in the probability of severe air pollution associated with certain extreme air pollution meteorological events.

We note that the U.S. anthropogenic emissions declined during the 2001-2010 period which has important implications for air quality. But we do not expect these emission changes to have any significant impacts on the derived sensitivities of air quality to extreme air pollution meteorology since a) our derived air quality sensitivities to extreme meteorology are expressed as relative (percentage) changes; and b) the 10-yr period is a relatively short time window in the context of global climate change therefore we expect the climate-induced changes in extreme air pollution meteorology should be small during this period. We have performed additional analyses to confirm that our derived sensitivities are not affected by emission changes.

2.4 Results and discussion

We first examine the evolution of extreme air pollution meteorology in the past six decades. We follow the World Meteorological Organization method [*Frich et al.*, 2002] on the definition of heat waves with some modification - A heat wave is defined when the daily maximum temperature at a given location exceeds the climatological" daily maximum temperature (averaged over the reference period of 1961-1990) by at least 5 K for more than two consecutive days. Figure 2.1a shows the average annual occurrences of heat waves in the first 30-year (1951-1980) period as well as the percentage changes when compared with the more recent 30-year (1981-2010) period. Significant increases in heat waves in the more recent decades are observed over most continental regions, especially the high latitude regions. For most regions, the trends in the frequency of heat waves are similar to those identified in the literature [*Frich et al.*, 2002]. It is noticeable that the frequency of heat waves have decreased over some areas in the United States in the past decades. The annual average frequency of heat waves for the global non-polar continental regions is found to increase by 25.8±3.3% (Table 2.1). The largest increases (around 40%) are found during Northern Hemisphere spring (March-May) and summer (June-August) seasons.

For temperature inversions, we examine the atmospheric temperature profile below 800 hPa which is most relevant to air quality. A temperature inversion event is defined

Table 2.1
The percentage change ± standard error of the mean (SEM) (%) in the average frequencies of extreme events (HW: heat waves; TI: temperature inversions; AS: atmospheric stagnation episodes) for the global non-polar continental regions between the two 30-yr periods: 1981-2010 vs. 1951-1980. * indicates statistically non-significant results at the 95% confidence interval.

Event	Season	Global	Northern Hemisphere
HW	Annual	25.8 ± 3.3	24.5 ± 3.1
	March-May	45.4 ± 4.3	44.9 ± 4.1
	June-August	40.3 ± 5.0	40.9 ± 5.3
	September-November	9.9 ± 3.6	$6.5 \pm 3.7*$
	December-January	17.9 ± 3.5	16.2 ± 3.3
TI	Annual	6.2 ± 3.2	$6.7 \pm 3.4*$
	March-May	9.1 ± 3.9	9.0 ± 4.3
	June-August	$10.3 \pm 5.3*$	17.4 ± 7.0
	September-November	8.8 ± 3.6	10.6 ± 3.9
	December-January	$1.8 \pm 3.4*$	$1.6 \pm 3.0*$
AS	Annual	4.5 ± 0.8	6.8 ± 0.9
	March-May	7.2 ± 0.9	9.8 ± 1.1
	June-August	6.7 ± 1.1	11.8 ± 1.3
	September-November	3.6 ± 0.9	5.5 ± 1.0
	December-January	$0.5 \pm 0.9*$	$1.0 \pm 1.1*$

when the temperature at a higher level is at least 0.1 K higher than the temperature below. On a global scale, a general increase in the occurrences of temperature inversions is found, except over the high latitudes Figure 2.1b. A warmer climate is expected to increase the evapotranspiration, releasing more latent heat in the upper

troposphere which could reduce the temperature lapse rate in the troposphere, especially over the tropics and mid-latitude regions. As a consequence, the atmospheric stability is generally expected to increase with climate change leading to more temperature inversions. On the other hand, the decreases in temperature inversions over polar regions reflect the strong surface warming there in the past decades, partly driven by the positive feedback associated with snow/ice albedo [*Houghton et al.*, 2001]. For non-polar continental regions in the Northern Hemisphere, the trends in temperature inversion events show clear seasonal variations: the strongest increases are observed in summer (by $17.4 \pm 7.0\%$) while little changes are found in winter.

The definition of atmospheric stagnation used in this study follows the National Climatic Data Center (NCDC) methodology [*Horton et al.*, 2012] with a relative threshold to focus on the local changes: A stagnation episode is defined when the 10 m wind speed, 500 hPa wind speed, and precipitation at a given location are all less than their climatological values for the reference period (1961-1990) by at least 20%. Figure 2.1c shows that the occurrences of atmospheric stagnation episodes have increased over most continental areas. Our results are consistent with Wang et al. [*Wang et al.*, 1999] who studied the changes in atmospheric stagnation episodes over the U.S. region during the past decades. For non-polar continental regions, the annual average atmospheric stagnation events have increased by $4.5 \pm 0.8\%$. This increase is partly due to the weakening of surface winds driven by climate change [*Vautard*

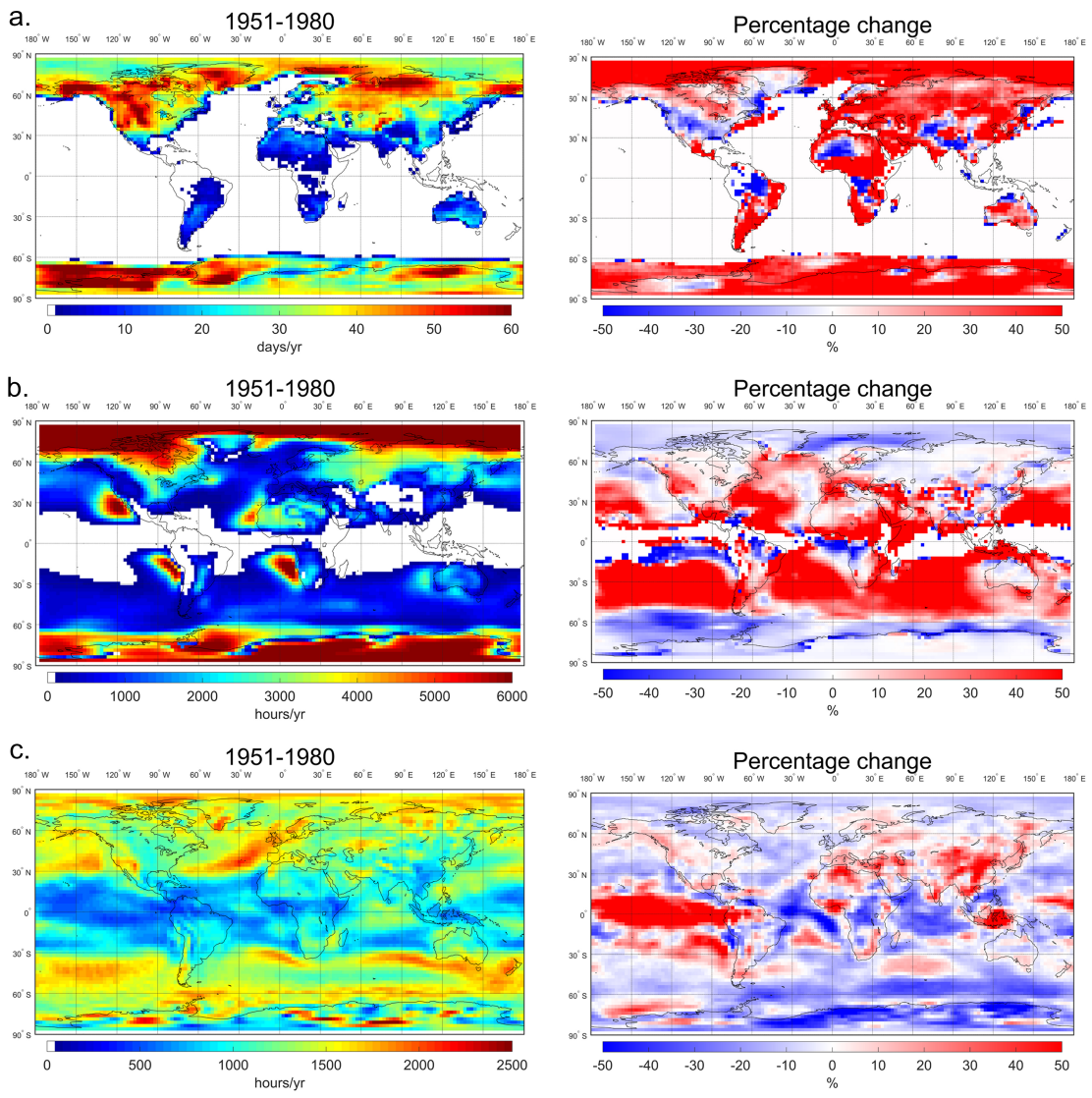

Figure 2.1: Changes in the frequency of extreme air pollution meteorological events in the past six decades (based on the NCEP reanalysis data): a. heat waves (days/yr); b. temperature inversions (hrs/yr); c. atmospheric stagnation episodes (hrs/yr). Left: 1951-1980 average; right: percentage change (%) between 1951-1980 and 1981-2010.

et al., 2010]. In addition, the more intense but less frequent precipitation in a warmer climate could also contribute to the increased frequency of atmospheric stagnation events [*Trenberth*, 2011].

It should be mentioned that we have applied various metrics for identifying each air pollution meteorological event and find no evidence of significant impacts on our results. For example, we use different definitions for stagnation episodes, including a) If the 10 m wind speed, 500 hPa wind speed, and precipitation at a given location are all less than their climatological values for the reference period (1961-1990) by at least 20% (the one currently being used in the dissertation); b) If the 10 m wind speed, 500 hPa wind speed, and precipitation at a given location all fall in the lowest 20% when compared to the distributions of these variables for the reference period (1961-1990). They lead to similar results on both the spatial variations and temporal trends in stagnation events, so we finally settle on the one currently used in the dissertation which appears most straightforward for the readers to understand. Similarly, we have tried various definitions for heat waves such as exceeding the climatological value by certain degrees or by a certain percentage, and there were little differences in the identified trends.

We have also compared the NCEP reanalysis data with the MERRA data [*Rienecker et al.*, 2011] for cross-referencing. Due to the limit of computing resources, we have only been able to process 10 years of MERRA data (1981-1985 and 2006-2010). We compare results from these two datasets based on 5-year averages: 2006-2010 vs. 1981-1985. Figure 2.2 to 2.4 show the side-by-side comparison of the spatial distributions of extreme air pollution meteorological events identified based on these two datasets. The frequencies of extreme air pollution meteorological events over different

continental regions are summarized in Table 2.2. In most cases, analyses based on these two databases show the same direction in long-term trends. However, significant differences between these two databases are identified for some regions (e.g., heat waves over South America; temperature inversions over the Southern Oceans). This reflects the uncertainties associated with these databases that we are not able to quantify in this study. On the other hand, it is reassuring to see that these two datasets are generally consistent in identifying the trends of extreme air pollution meteorology over continental regions where we have concerns of air pollution (30°N-60°N).

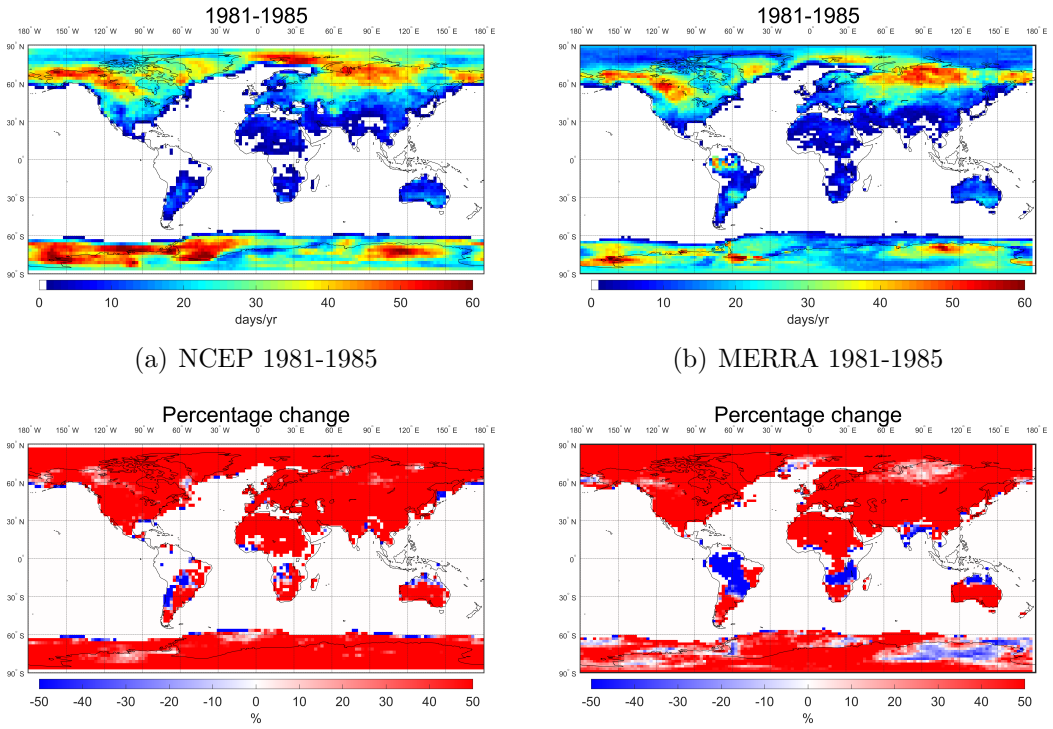

(a) NCEP 1981-1985

(b) MERRA 1981-1985

(c) NCEP percentage change

(d) MERRA percentage change

Figure 2.2: Long-term trends (2006-2010 vs. 1981-1985) in heat waves (days/yr) based on the NCEP reanalysis compared with the MERRA data. Top: 1981-1985 average; bottom: percentage change (%) between 1981-1985 and 2006-2010; left: NCEP data; right: MERRA data.

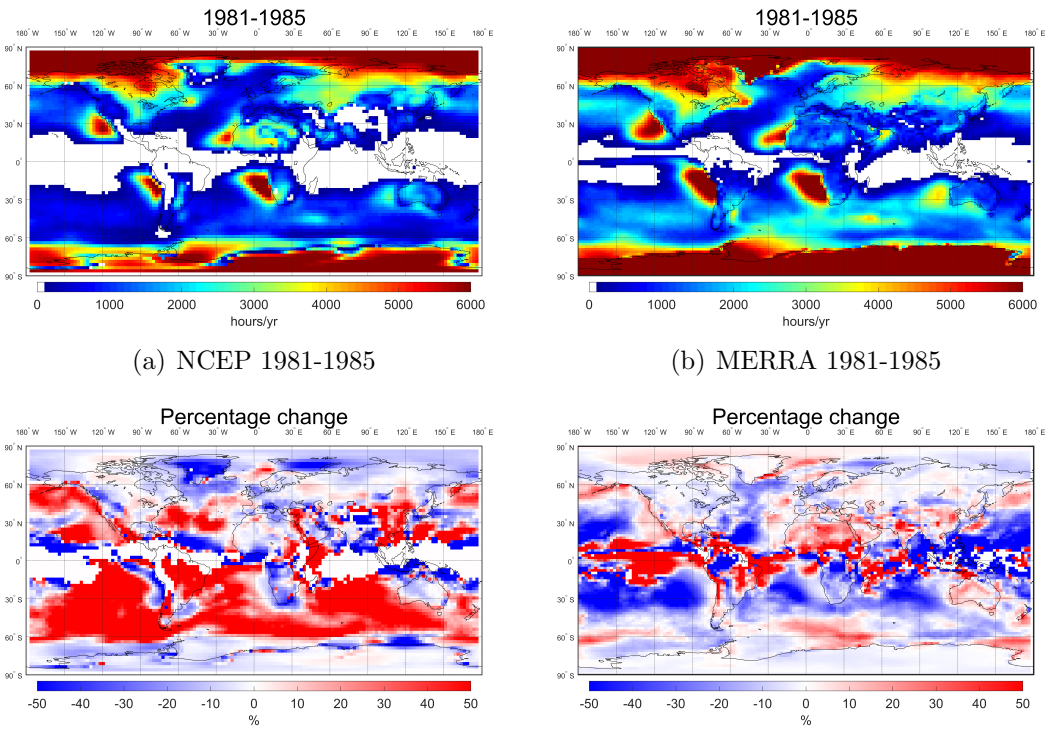

(a) NCEP 1981-1985

(b) MERRA 1981-1985

(c) NCEP percentage change

(d) MERRA percentage change

Figure 2.3: Long-term trends (2006-2010 vs. 1981-1985) in temperature inversions (hrs/yr) based on the NCEP reanalysis compared with the MERRA data. Top: 1981-1985 average; bottom: percentage change (%) between 1981-1985 and 2006-2010; left: NCEP data; right: MERRA data.

To examine the impacts on air quality from each specific extreme meteorological event (heat waves, temperature inversions or atmospheric stagnation episodes), we analyze air quality data from the U.S. EPA AQS database for 2001-2010 together with the meteorology data for the same period. The air quality data are processed into the same spatial resolution as the meteorology data ($2.5° \times 2.5°$) by averaging the available data from all the sites within the same grid cell. Daily average concentrations of $PM_{2.5}$ and afternoon (1-4pm local time) average concentrations of ozone (derived from hourly ozone data) are used in the analysis.

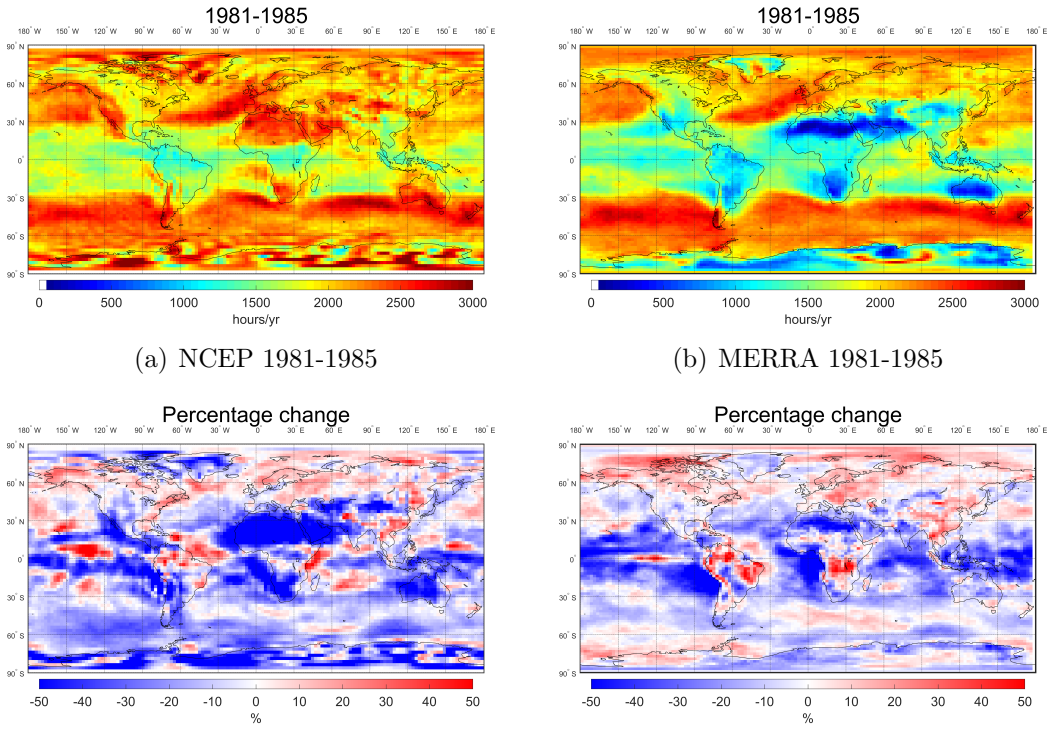

(a) NCEP 1981-1985

(b) MERRA 1981-1985

(c) NCEP percentage change

(d) MERRA percentage change

Figure 2.4: Long-term trends (2006-2010 vs. 1981-1985) in atmospheric stagnation episodes (hrs/yr) based on the NCEP reanalysis compared with the MERRA data. Top: 1981-1985 average; bottom: percentage change (%) between 1981-1985 and 2006-2010; left: NCEP data; right: MERRA data.

We first compare the monthly average air quality on event days with those on non-event days (Figure 2.5). The event groups tend to have much higher concentrations of ozone than no-event groups in warm seasons, with enhancements up to 20%. Figure 2.5a and Figure 2.5b shows that the highest sensitivity of surface ozone to temperature inversions and heat waves are found during summer and fall. In winter, when temperature inversion or heat waves happened, the concentrations of ozone are usually lower than days without these extreme events, which may reflect the weaker photochemical ozone production in those seasons [*Jacob et al.*, 1995; *Carmichael et al.*, 1998]. The

Table 2.2
The percentage change ± SEM (%) in the annual average frequencies of extreme events (HW: heat waves; TI: temperature inversions; AS: atmospheric stagnation episodes) for the long-term trends (2006-2010 vs. 1981-1985) in different continental regions based on the NCEP reanalysis data compared with the MERRA data (∗ indicates statistically non-significant results at the 95% confidence interval)

Regions	Data	HW	TI	AS
90°N-60°N	NCEP	95.9 ± 3.9	-6.7 ± 2.4	$0.9 \pm 1.7*$
	MERRA	105.9 ± 8.4	$-1.8 \pm 2.5*$	6.2 ± 2.8
60°N-30°N	NCEP	195.5 ± 6.3	$0.6 \pm 3.1*$	-10.2 ± 0.9
	MERRA	201.9 ± 13.8	$-1.3 \pm 2.1*$	$-1 \pm 1.1*$
30°N-0°	NCEP	321 ± 25.7	$-0.9 \pm 6.9*$	-36.4 ± 1.2
	MERRA	425.3 ± 68.4	$2.5 \pm 6.6*$	-16.1 ± 1.3
0°-30°S	NCEP	158.2 ± 21	$-0.9 \pm 8.1*$	-24 ± 1.1
	MERRA	107.1 ± 29.2	$-9.5 \pm 6.3*$	-20.1 ± 1.0
30°S-60°S	NCEP	84.8 ± 18.7	$3.1 \pm 11.2*$	-25.8 ± 2.3
	MERRA	98.9 ± 34.1	-7.9 ± 1.9	-5.1 ± 0.8
60°S-90°S	NCEP	107.2 ± 6.6	$-5.3 \pm 3.0*$	-32.7 ± 2.1
	MERRA	29.5 ± 4.8	$-0.3 \pm 2.5*$	$-4.7 \pm 3.5*$

impacts of extreme events on $PM_{2.5}$ are always positive but show less seasonal patterns. Heat wave group tends to have less concentration of $PM_{2.5}$ than no heat wave group in the winter time.

We then compare the air quality for event group with those for the no-event group in each grid box (Figure 2.6) to study the spatial distribution of sensitivities. The statistical significance of the differences between these two groups are evaluated with

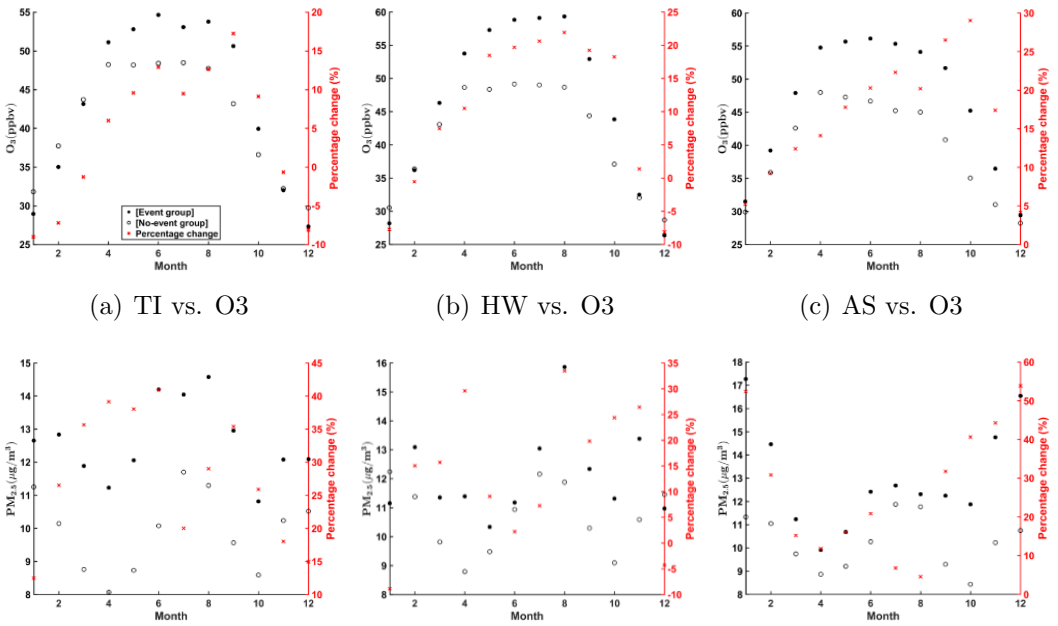

(a) TI vs. O3 (b) HW vs. O3 (c) AS vs. O3

(d) TI vs. PM (e) HW vs. PM (f) AS vs. PM

Figure 2.5: Monthly average concentrations of air pollutants for event group and the no-event group over the United States. Percentage changes show the enhancements in the monthly average air pollutant concentrations by extreme meteorological events.

t-tests with a 95% confidence interval. Figure 2.6a shows the percentage change of seasonal average afternoon ozone concentrations on days with heat waves compared to those on days without heat waves for each season. There are large spatial variations in the sensitivity of ozone to heat waves. The strongest sensitivities are found in the eastern United States and the west coast, where the mixing ratios of afternoon ozone are enhanced by more than 40% on days with heat waves, reflecting the strong emissions of ozone precursors [*Jacob et al.*, 1993] and hence high ozone production there. As discussed above, the frequency of heat waves have decreased in the past decades over some areas in the United States (Figure 2.1a), which could have canceled

out some of the increases in high ozone pollution risk induced by other factors over those areas in the past decades.

We find that heat waves have much stronger impacts on air quality than single hot days with the same temperature. Figure 2.7 shows the response of summer ozone concentrations to temperature, one group for all days in the season, another only for days with heat waves. We can see that with the same temperature, ozone concentrations on days with heat waves are significantly higher than those non-consecutive hot days, especially over the 293-313K temperature range. Generally, the ozone concentrations on days with heat waves are more than 4.5 ppb higher than those projected by the average ozone-temperature correlation. This reflects the build-up effects from the extended period of high temperature during heat wave events. On the other hand, the heat wave effects appear weaker when the temperature is above 313K (Figure 2.7). In comparison, *Steiner et al.* [2010], based on observational data from California, reported that the daily maximum ozone is most sensitive to temperature in the range of 295-312K but the ozone formation is suppressed when the temperature is above 312K.

The impacts of temperature inversions on seasonal average concentrations of $PM_{2.5}$ are shown in Figure 2.6b. The strongest impacts from temperature inversions are observed in winter time with daily average $PM_{2.5}$ concentrations enhanced by 40% or more over large areas in the United States. The impacts are much weaker in

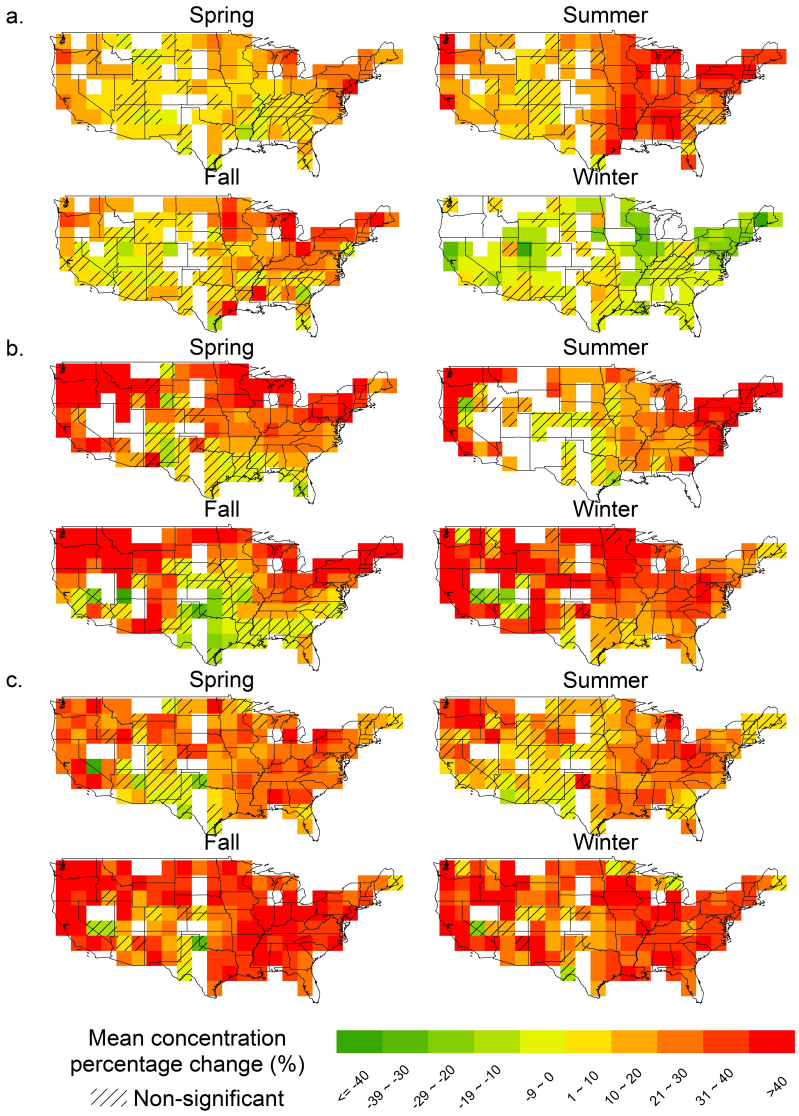

Figure 2.6: Enhancements in the seasonal average air pollutant concentrations by extreme meteorological events, shown as the percentage change (%) of mean concentrations (for either ozone or $PM_{2.5}$) on days with a specific meteorological event (event groups) compared to those on days without that event occurrence (no-event groups): a. ozone vs. heat waves; b. $PM_{2.5}$ vs. temperature inversions; c. $PM_{2.5}$ vs. atmospheric stagnation episodes. Shadowed regions indicate that the differences between the two groups are statistically non-significant at the 95% confidence interval. Blank regions indicate those with less than 3 data points for either group.

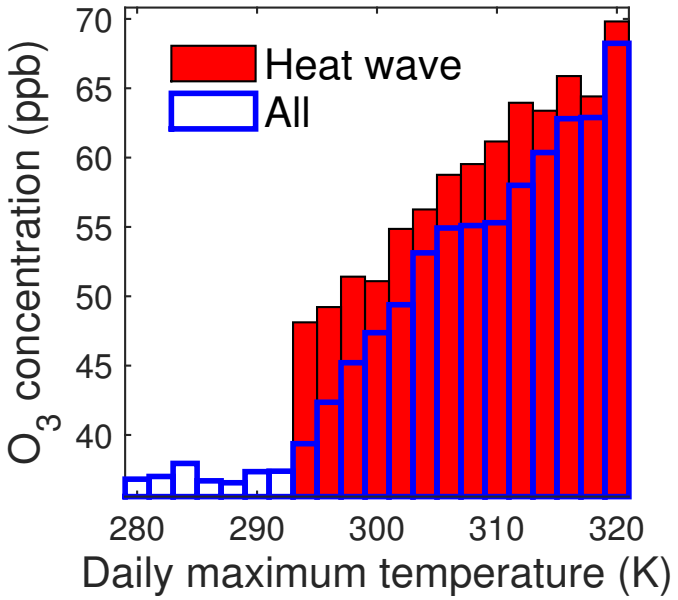

Figure 2.7: Summer ozone concentrations as a function of daily maximum temperature based on 2001-2010 data in the United States. The blue curve shows the average ozone concentrations for all the days with temperature falling in specific temperature bins while the red curve only covers days with heat waves.

summer and fall, mainly limited to the northeast and northwest states. In contrast, significant impacts on $PM_{2.5}$ concentrations associated with atmospheric stagnation episodes are found for all seasons throughout the United States (Figure 2.6c), with the largest increases in $PM_{2.5}$ concentrations exceeding 40% over large areas.

We also carry out additional analysis by using the MERRA data instead of the NCEP data to examine the impacts on air quality from extreme air pollution meteorology. As we can see from Figure 2.8 and 2.9, these two datasets show essentially the same sensitivity of air quality (for both ozone and PM) to extreme meteorological events for 2006-2010.

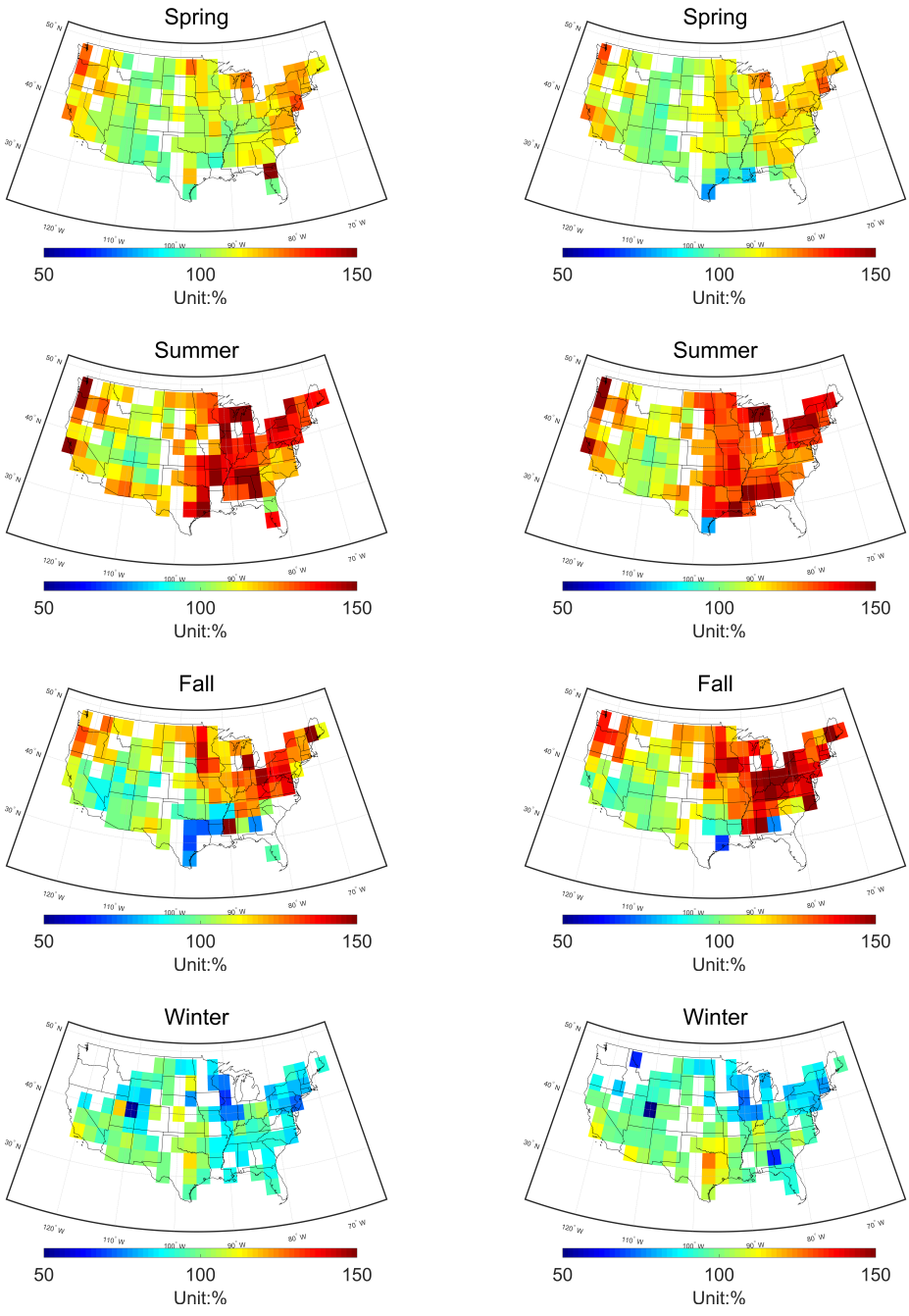

Figure 2.8: Impacts of heat waves on ozone in the United States (shown as the ratio of ozone concentrations on days with heat waves and those without heat waves) based on NCEP vs. MERRA data (2006-2010). Left: NCEP data; right: MERRA data.

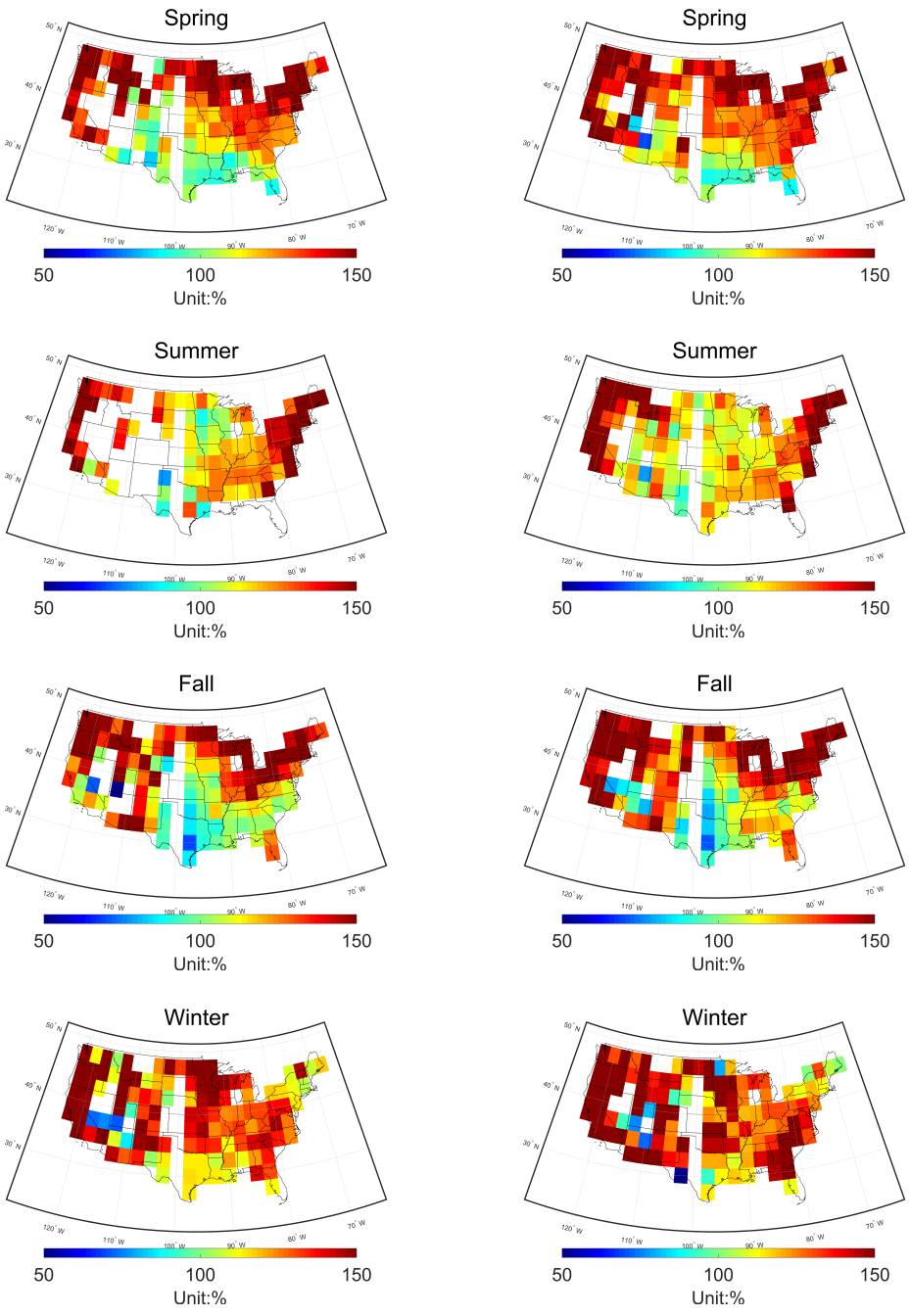

Figure 2.9: Impacts of temperature inversions on $PM_{2.5}$ in the United States (shown as the ratio of $PM_{2.5}$ concentrations on days with temperature inversions and those without temperature inversions) based on NCEP vs. MERRA data (2006-2010). Left: NCEP data; right: MERRA data.

There have been significant changes in the anthropogenic emissions of ozone and $PM_{2.5}$ precursors during the 2001-2010 period (detailed information available from the U.S. EPA - https://www.epa.gov/air-emissions-inventories/air-pollutant-emissions-trends-data). These changes could affect the derived sensitivity of air quality to extreme meteorological events if there has been any significant trends in air pollution meteorology during the same period and these trends correlate with the emission change. However, the 10-year period is a relatively short time frame in the context of global climate change so we expect the climate-induced changes in extreme air pollution meteorology are small during this period. Therefore we do not expect the emission changes to have any significant impacts on the derived sensitivities when the sensitivities are expressed as the relative (percentage) changes. Nevertheless, we have carried out two additional tests to further confirm that the derived sensitivities are not affected by emission changes.

For the first test, we separate the 10-yr data into 2 groups of 5-yr data (2001-2005 and 2006-2010 respectively). We found the sensitivities of air quality to extreme meteorological events derived based on these two groups are very close and they do not show any significant differences. For example, in summer, the enhancement in the mean concentration of ozone due to heat waves is around 20% for both groups (19.84% for the 2001-2005 group and 20.36% for the 2006-2010 group).

For the second test, we processed the air quality data into detrended data to eliminate

the effects from emission changes. We apply a least square linear regression to the original air quality data

$$y_i^{'} = \alpha + \beta t_i \tag{2.5}$$

where α and β are coefficients of the linear regression and $y_i^{'}$ is the trend data for air quality at time t_i. The detrended air quality d_i is calculated as

$$d_i = y_i - y_i^{'} + \bar{y} \tag{2.6}$$

where y_i is the original air quality data at time t_i and $\bar{y}$ is the average of original air quality data. When we compare the enhancements in air pollution by extreme events derived based on the original air quality data to those derived based on the detreneded data, we find they are essentially the same. For example, for the enhancement in summer ozone due to heat waves, we find that the results only differ by 0.51% and for summer $PM_{2.5}$ they only differ by 0.05%. Therefore we believe these two tests further confirm that the emission changes during this period do not have any significant impacts on the derived sensitivities of air quality to extreme air pollution meteorology.

We verify the capability of a chemical transport model (GEOS-Chem) in simulating the relationship between extreme events and air quality. By calculating the ratio between seasonal average ozone concentrations in event group and the ones in no-event group (Figure 2.10, 2.11, and 2.12), we compare the impacts of extreme air pollution meteorological events on ozone concentrations simulated from GEOS-Chem with the

observation (NCEP and AQS databases). Limited by the GEOS5 meteorological data used as meteorological input data in GEOS-Chem, the comparison focuses on the 2004-2012 period. Temperature inversions (Figure 2.10) show weaker correlation with ozone concentration in simulation results than observations, which could be due to the simplified boundary layer mixing mechanism in the GEOS-Chem model. In contrast, other extreme events are comparable with the observational analysis result. For spring, summer, and fall, the model clearly captured the spatial distribution of the mean concentration ratio between heat wave group and no heat wave group (Figure 2.11) that the eastern regions in the United States have a stronger response to the occurrences of heat waves than the western regions.

We further examine the impacts of extreme air pollution meteorology on the cumulative probability distributions of ozone and $PM_{2.5}$ concentrations (Figure 2.13). For each season, the cumulative probability distributions of ozone mixing ratios for days with heat waves were compared with those without heat waves (Figure 2.13a). We can see that extreme air pollution meteorology usually has the greatest impacts on the high end of the distributions, which represent the high pollution episodes. For example, during summer time, the 95th percentile ozone is increased by about 25% while the 50th percentile ozone is only increased by about 19% due to heat waves. Similar feature is found for the impacts on $PM_{2.5}$ from temperature inversions and atmospheric stagnation episodes. In winter time, the 95th percentile $PM_{2.5}$ concentration is increased by 65% while the 50th percentile $PM_{2.5}$ concentration only increases

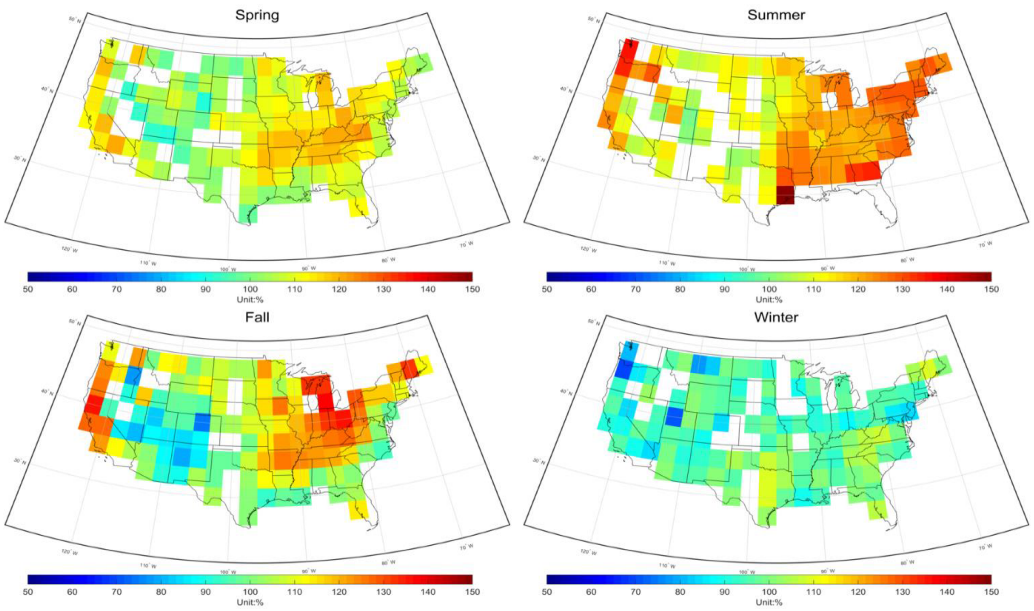

(a) Observations

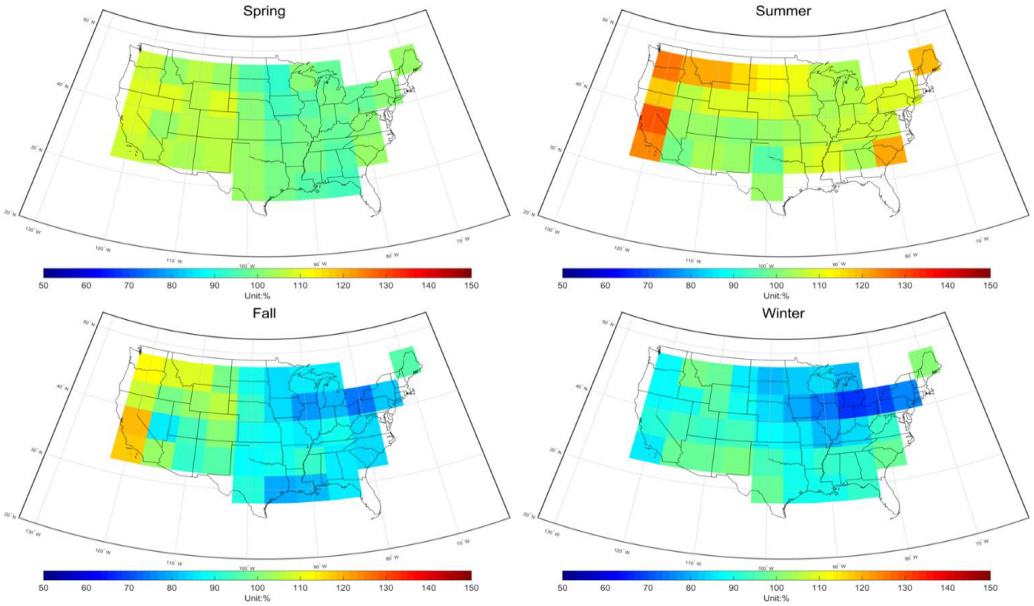

(b) Simulations

Figure 2.10: Enhancements in the seasonal average air pollutant concentrations by temperature inversions during the 2004-2012 period, shown as the ratio of mean concentrations for ozone on days with temperature inversions compared to those on days without temperature inversions. (a) observation results based on NCEP and AQS database; (b) simulation results based on GEOS-Chem v9-02-01. Blank regions indicate those with less than 3 data points for either group.

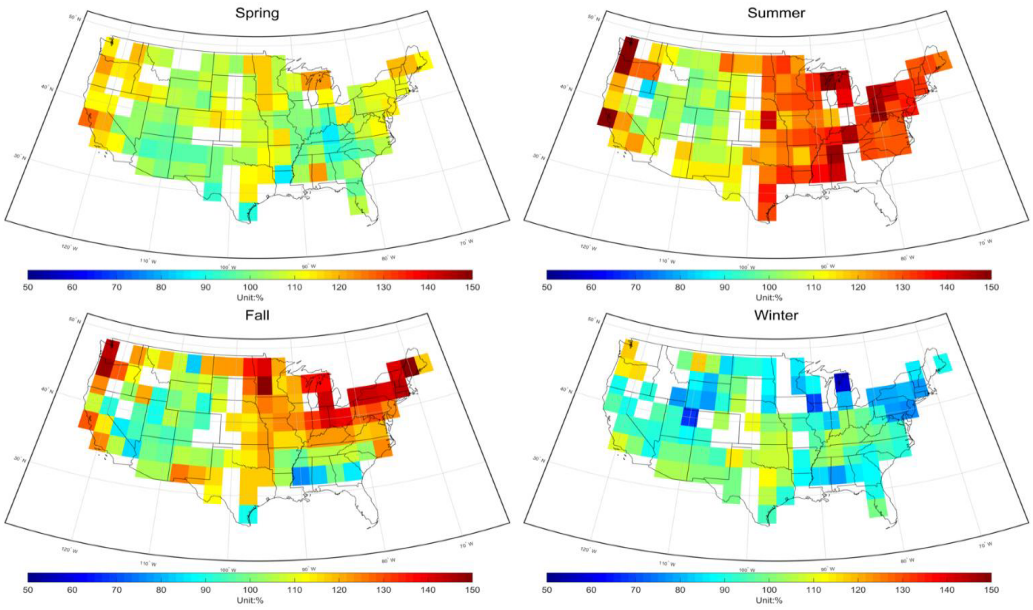

(a) Observations

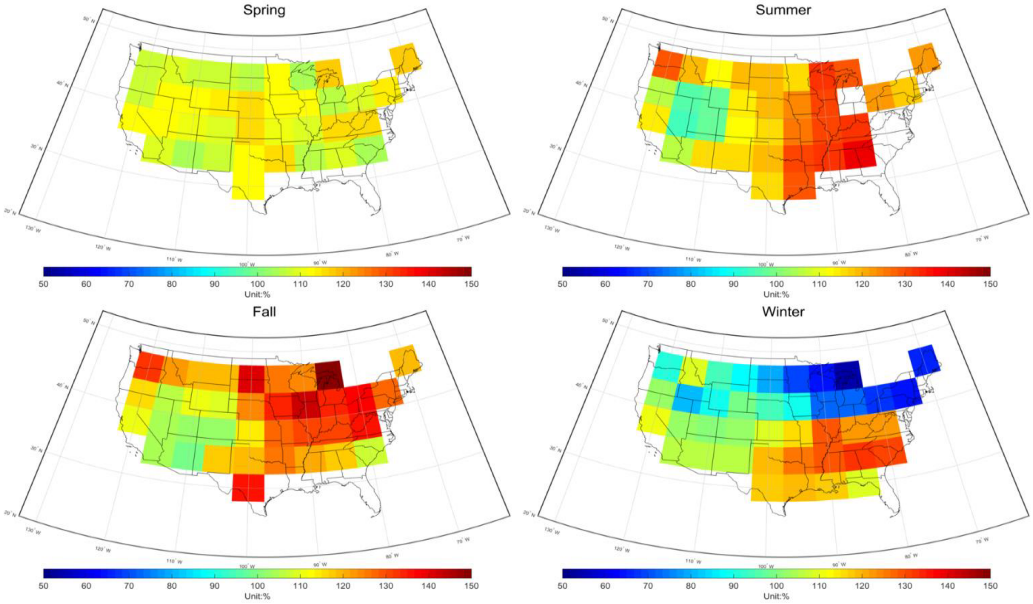

(b) Simulations

Figure 2.11: Enhancements in the seasonal average air pollutant concentrations by heat waves during the 2004-2012 period, shown as the ratio of mean concentrations for ozone on days with heat waves compared to those on days without heat waves. (a) observation results based on NCEP and AQS database; (b) simulation results based on GEOS-Chem v9-02-01. Blank regions indicate those with less than 3 data points for either group.

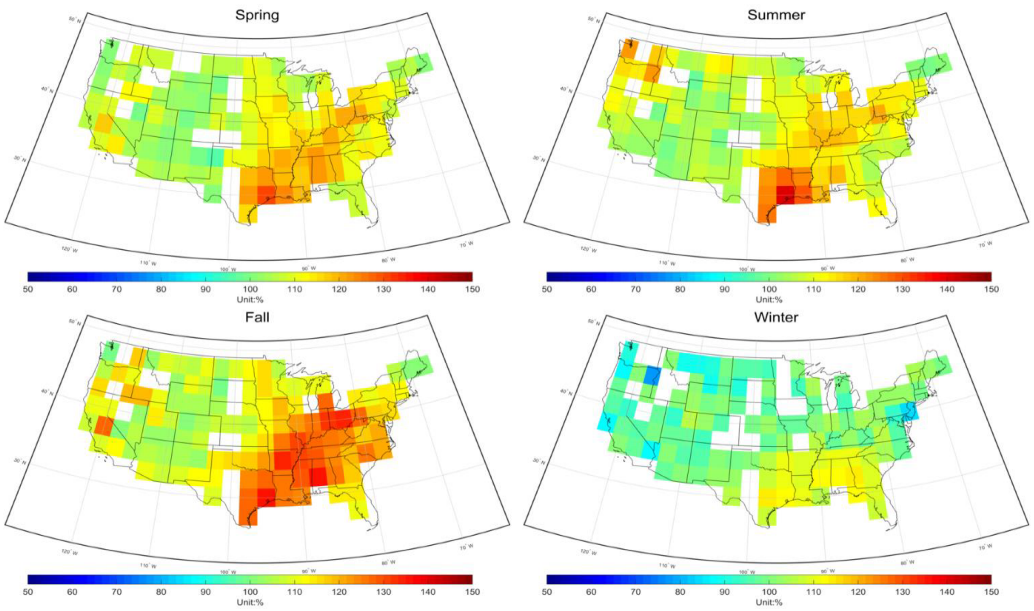

(a) Observations

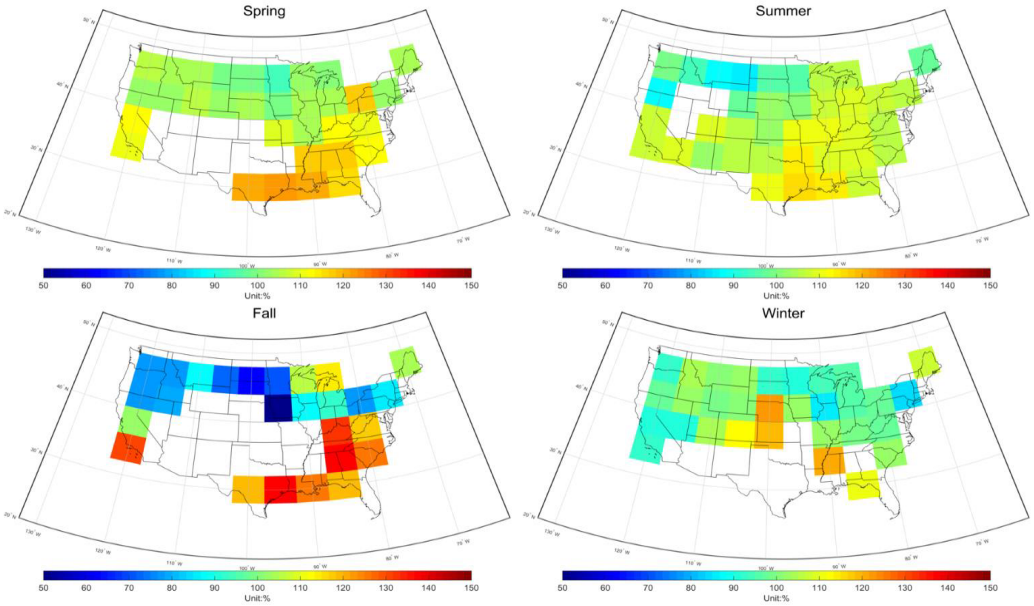

(b) Simulations

Figure 2.12: Enhancements in the seasonal average air pollutant concentrations by atmospheric stagnation episodes during the 2004-2012 period, shown as the ratio of mean concentrations for ozone on days with atmospheric stagnation episodes compared to those on days without atmospheric stagnation episodes. (a) observation results based on NCEP and AQS database; (b) simulation results based on GEOS-Chem v9-02-01. Blank regions indicate those with less than 3 data points for either group.

by 28% in response to temperature inversions (Figure 2.13b). Similarly, atmospheric stagnation episodes are found to have little effects on the low end of $PM_{2.5}$ distributions (which represent the clean conditions) but significant impacts on the high pollution episodes for each season (Figure 2.13c).

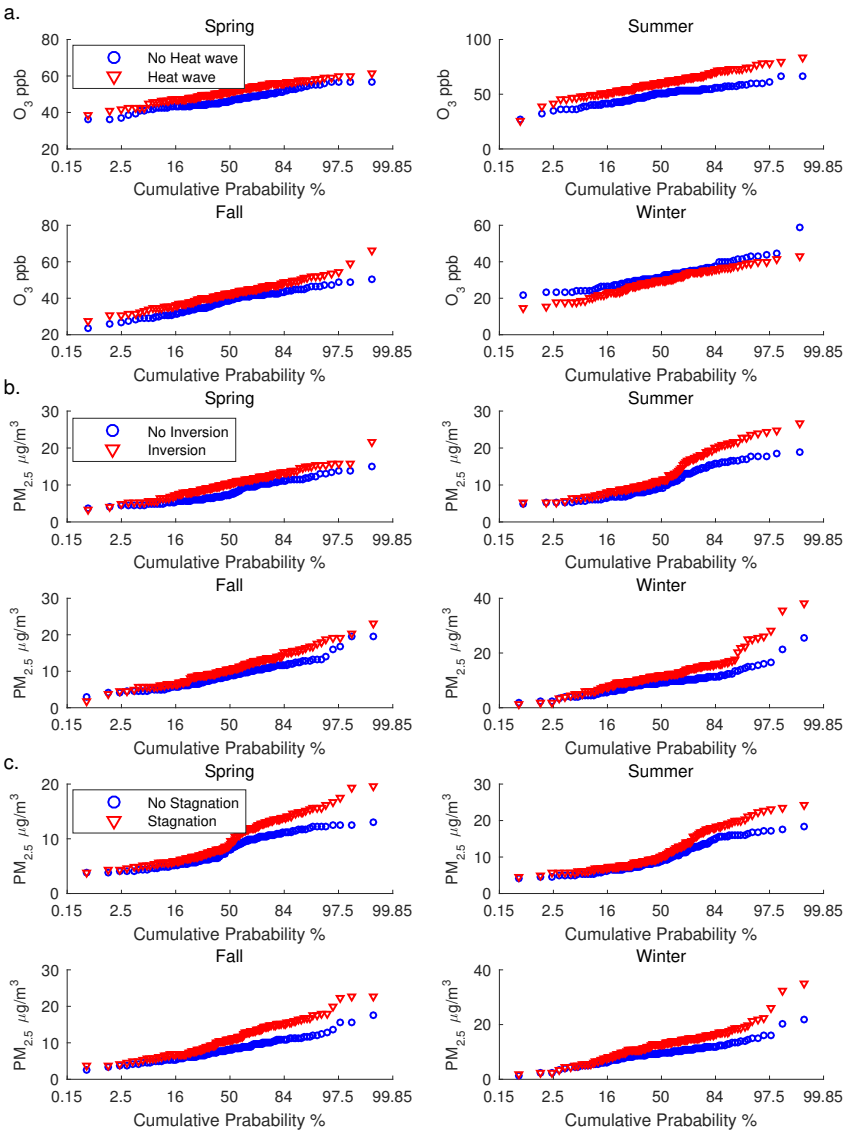

Figure 2.13: Cumulative probability plots for concentrations of air pollutants. Red triangle: event group; blue circle: no-event group. a. ozone mean concentrations of heat wave group and no heat wave group; b. $PM_{2.5}$ mean concentrations of temperature inversion group and no temperature inversion group; c. $PM_{2.5}$ mean concentrations of atmospheric stagnation group and no atmospheric stagnation group.

For a specific air pollutant (i.e. ozone or $PM_{2.5}$), we define the high pollution days as the top 10% most polluted days for each season and examine their sensitivities to various extreme air pollution meteorological events. To better quantify the impacts from extreme events on high pollution episodes and their relative importance, we define an impact factor as the enhancement in the probability of high pollution episodes due to extreme meteorological events (see Section 2.3 for details). The impact factors for high ozone pollution days in summer associated with the three types of extreme events on state level are shown in Figure 2.14a and 2.14c and similarly the impact factors for different regions in the United States are shown in Figure 2.14b and 2.14d.

We find that heat waves are the most important meteorological event in leading to high ozone pollution days in summer for most areas in the United States (Figure 2.14a and 2.14b). The impact factors for ozone pollution associated with heat waves are particularly high in the eastern United States (such as Louisiana, Alabama and Georgia), with values up to 6, which indicates the probability of severe ozone pollution would be enhanced by a factor of 7 when there are heat waves over those areas. The large spatial variations in the impact factors reflect the regional variations in anthropogenic and natural emissions of air pollutants and their precursors, climate, orography and geography (such as whether downwind or upwind of major air pollutant source regions). The highest impact factors for temperature inversions are found over the eastern United States and the Northwest region, while the highest impact factors for atmospheric stagnation episodes are found over the Midwest.

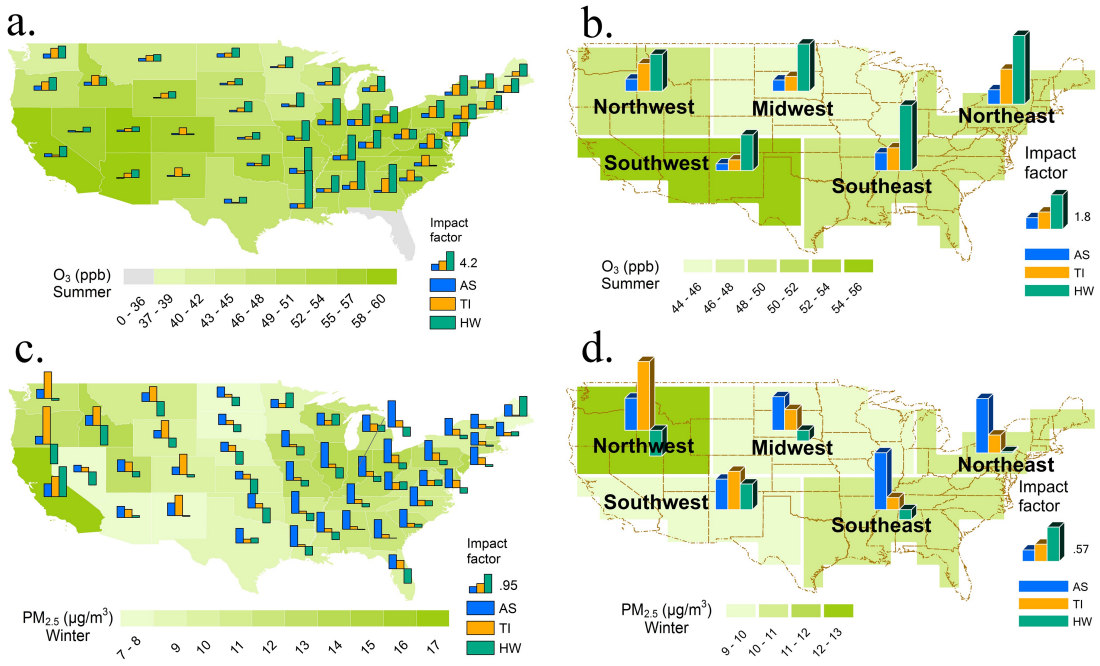

Figure 2.14: Enhancements in the probability of high pollution episodes by extreme air pollution meteorological events for different states and regions in the United States, shown as the impact factor for (a) summer ozone by state; (b) summer ozone by region; (c) winter $PM_{2.5}$ by state; and (d) winter $PM_{2.5}$ by region associated with various meteorological events (heat waves, temperature inversions and atmospheric stagnation episodes; indicated by the green, orange, and blue bars respectively). The impact factor is defined as the enhancement in the probability of high pollution episodes due to extreme meteorological events. Background color indicates the mean concentration for that pollutant. Bar plots for the four smallest states (includes District of Columbia, Rhode Island, Delaware, and Connecticut) are omitted to increase accessibility.

Figure 2.14c and 2.14d shows the impact factors for $PM_{2.5}$ in winter associated with the three types of extreme events. The highest impact factors (up to 1.6) are found for temperature inversions over the western regions. The impact factors for atmospheric stagnation episodes are generally higher in the eastern United States, and consistently positive (indicating positive correlation between stagnation episodes and high $PM_{2.5}$ pollution episodes) throughout the United States. In contrast, some negative impact

factors are found for heat waves. One likely reason is the decrease of ammonium nitrate (a major component of $PM_{2.5}$ in winter time) at higher temperatures. This hypothesis is supported by the decrease of high nitrate days when heat waves occur as shown in Figure 2.15. In addition, during warmer days in winter, there would be less residential biomass burning, which is a major source for aerosols in the Western United States [*Chen et al.*, 2012]. This could also contribute to the negative correlation between heat waves and $PM_{2.5}$ in winter.

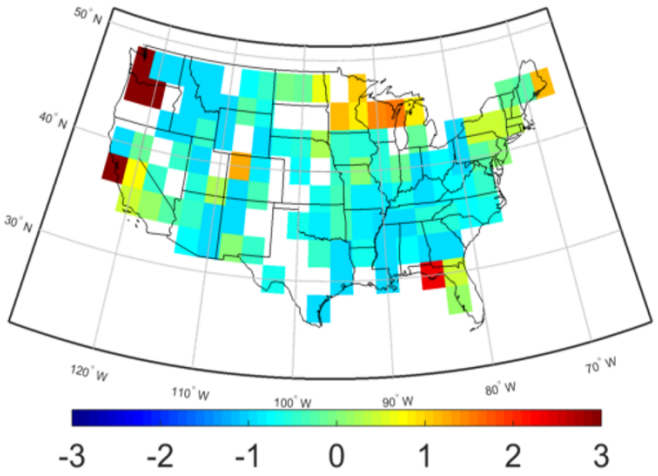

Figure 2.15: Impact factor for nitrate in winter (2001-2010) that associated with heat wave, based on the AQS database.

For the locations with extreme meteorological events identified, we find that on average there are about one third of the times (32% as shown in Table 2.3) with more than one extreme events occurring simultaneously. To account for the interactions between different types of extreme meteorological events and their synthetic effects on air quality, we also calculate the impact factors for high pollution days associated

with multiple events occurring simultaneously. The impact factors for U.S. high ozone and $PM_{2.5}$ days in different seasons are summarized in Table 2.4. With the increase in the number of simultaneously occurring extreme events (from 0-3), the probability of high pollution episodes almost always increases (with the notable exception of the winter season). The highest impact factor (3.3) is found for summer ozone associated with the combination of three extreme events. This implies that, on average over the whole United States, the probability of high ozone pollution would be enhanced by more than a factor of 4 compared to the seasonal average when the three extreme events occur at the same time in summer.

Table 2.3
Number of extreme air pollution meteorological events identified over the U.S. region for the 2001-2010 period (HW: heat waves; TI: temperature inversions; AS: atmospheric stagnation episodes).

	None	Single event		
		Only HW	Only TI	Only AS
number	38349	3048	14274	13753
total	38349	31075		
	Multiple events			
	HW & TI	HW & AS	TI & AS	All
number	1902	2688	8151	1794
total	14535			

Table 2.4

The impact factor for high pollution days (ozone and $PM_{2.5}$) over the United States associated with various extreme meteorological events (None: no event; HW: only heat waves; TI: only temperature inversions; AS: only atmospheric stagnation episodes; All: three kinds of events happened at the same time). High pollution days are defined as the top 10% most polluted days for each season during 2001-2010. The impact factor is defined as the enhancement in the probability of high pollution episodes due to extreme meteorological events.

Species	Season	None	HW	TI	AS	HW & TI	HW & AS	TI & AS	All
O3	Spring	-0.5	0.1	0.0	0.0	1.2	1.0	1.1	3.0
	Summer	-0.5	1.2	0.4	0.2	3.0	2.1	1.3	3.3
	Fall	-0.5	-0.1	-0.2	0.4	0.8	0.8	0.6	2.1
	Winter	0.1	-0.4	-0.1	0.2	-0.1	0.1	0.1	0.0
$PM_{2.5}$	Spring	-0.4	0.0	0.1	0.2	0.6	0.7	0.8	1.9
	Summer	-0.3	0.8	0.2	0.2	1.9	1.2	0.7	2.5
	Fall	-0.4	0.2	-0.3	0.4	1.0	1.0	0.5	2.0
	Winter	-0.5	-0.7	-0.1	0.2	-0.2	0.3	1.2	0.8

Chapter 3

Prediction of High Pollution Episodes with the Occurrences of Extreme Air Pollution Meteorological Events

The material contained in this chapter will be submitted to the *Geophysical Research Letter*. Hou, P., and S. Wu (2018), Prediction of high pollution episodes with the occurrences of extreme air pollution meteorological events, to be submitted.

3.1 Abstract

High pollution episodes, which are harmful to public health, can be affected by meteorology, especially extreme air pollution meteorological events. The strong correlation between extreme air pollution meteorological events and the high end of air pollution distribution makes the occurrences of these meteorological events good predictors to forecast the high pollution episodes. We develop statistical models to predict the high air pollution episodes of ozone and fine particulate matters ($PM_{2.5}$) with four types of extreme air pollution meteorological events. We find that the occurrences of heat waves, temperature inversions, and atmospheric stagnation episodes can explain more than 80% of the interannual variations in high ozone pollution episodes in the northeast US in summer. Besides, fire events affect southwest US most for both ozone and $PM_{2.5}$ in the summertime.

3.2 Introduction

Meteorology is an essential factor for air quality. Because meteorology has an impact on several processes related to air pollution, including emissions, chemistry, transport, and deposition [*Fiala et al.*, 2003; *Filleul et al.*, 2006; *Kinney*, 2008; *Leibensperger et al.*, 2008; *Ordóñez et al.*, 2010; **?**; *Steiner et al.*, 2010]. Some extreme meteorological

events, such as heat waves, temperature inversions, atmospheric stagnation episodes, and wildfire, are found to have stronger impacts on air quality [*Fiore et al.*, 2012; **?**]. These extreme events are named as extreme air pollution meteorological events in this study.

Extreme air pollution meteorological events are associated with high air pollution episodes which threaten the public health. In 1952 London Smog event, the high particulate matter (PM) episodes were related to the persistent temperature inversions and atmospheric stagnation episodes [*Laskin*, 2006]. A high ozone episode was triggered by the severe European heat wave in 2003, which was one of the main causes of more than 70,000 deaths in that event [*Robine et al.*, 2008; *Semenza et al.*, 1996]. Our observational analysis (NCEP, MERRA, and AQS) and model simulations (GEOS-Chem) in Chapter 2 showed that the occurrences of high pollution episodes increased when extreme air pollution meteorological events occurred in a large area of US [*Hou and Wu*, 2016]. These sensitivities can be applied to predict high pollution episodes with regression models.

Most previous studies predicted the concentrations of ozone and $PM_{2.5}$ using statistical models under normal meteorology conditions [*Abdul-Wahab et al.*, 2005; *Gupta and Christopher*, 2009; *Tai et al.*, 2012]. Only a few studies worked on the prediction of air quality during extreme meteorological events, yet they usually focused on only one type of extreme air pollution meteorology. *Shen et al.* [2016] predicted the ozone

concentration with daily maximum temperature. *Leibensperger et al.* [2008] predicted the high ozone episodes with the frequency of mid-latitude cyclones. *Balachandran et al.* [2017] predicted $PM_{2.5}$ during wildfire events. As far as we know, no one predicts high air pollution episodes with multiple types of extreme events. However, when multiple types of the extreme air pollution meteorological events happened at the same time, the probability of high pollution episodes would further increase in most cases [*Hou and Wu*, 2016]. With the impacts of the extreme air pollution meteorological events on high pollution episodes, we construct statistical models to predict the high pollution episodes of ozone and $PM_{2.5}$ with the occurrences of extreme air pollution meteorological events (heat waves, temperature inversions, atmospheric stagnation episodes, and wildfire) in two consecutive days. We use these statistical models to predict the high pollution period around the 2000s, and apply observational data (AQS) to evaluate the ability of our statistical models.

3.3 Methods

We construct regression models to predict the probability of high pollution episodes with the occurrences of extreme air pollution meteorological events. Heat waves, temperature inversions, and atmospheric stagnation episodes in two consecutive days are considered as independent variables in the model. Two series of regression analysis are made to predict high ozone episodes and high $PM_{2.5}$ episodes, respectively. Fire

events are also involved as independent variables in an extra test to discuss the impacts of fire on high pollution episodes.

We apply National Centers for Environmental Prediction (NCEP) reanalysis dataset [*Kalnay et al.*, 1996] (http://www.esrl.noaa.gov/psd/) to investigate the occurrences of heat waves, temperature inversions, and atmospheric stagnation episodes. The NCEP dataset has a spatial resolution of 2.5° longitude × 2.5° latitude and a temporal resolution of 6 hours. To match the temporal resolution of air pollutants, the occurrences of extreme air pollution meteorological events are calculated daily.

The definitions of extreme air pollution meteorological events are the same with the definitions shown in Chapter 2. A heat wave is defined when the daily maximum temperature at a given location exceeds the climatological daily maximum temperature (averaged over the reference period of 1961-1990) by at least 5 K for more than two consecutive days. A temperature inversion event is defined when the temperature at a higher level is at least 0.1 K higher than the temperature below for the atmospheric temperature profile below 800 hPa. A stagnation episode is defined when the 10 m wind speed, 500 hPa wind speed, and precipitation at a given location are all less than their climatological values for the reference period (1961-1990) by at least 20%.

We examine the fire events based on the Global Fire Emissions Database (GFED4) daily burned area (without small fires) database [*Randerson et al.*, 2015]

(http://www.globalfiredata.org), since the burned area (with small fires) only available in monthly, rather than higher temporal resolution. The database covers 2001-2015 with a spatial resolution of 0.25° longitude × 0.25° latitude. To match the resolution of NCEP database, the GFED4 database is regrided to 2.5° longitude × 2.5° latitude. A fire event is defined as a day with non-zero burned area in a given grid box.

The analysis of high pollution days is based on the U.S. Environmental Protection Agency (EPA) Air Quality System (AQS, http://www.epa.gov/airdata/) database. Since NCEP dataset has a horizontal resolution of 2.5° latitude by 2.5° longitude, the AQS dataset is processed into the same spatial resolution by averaging the available data from all the sites within the same grid cell. We focus on afternoon (1-4pm local time) concentrations for ozone (derived from hourly ozone data) and daily average concentrations for $PM_{2.5}$. The high pollution episodes are defined as the top 10% most polluted days for the years during the study period in each grid box. The study period is decided by the available of data, which is 1990-2015 for ozone, 1998-2015 for $PM_{2.5}$, and 2001-2015 for the analysis considered or compared with fire events.

A series of logistic regression models are built and applied to predict high pollution episodes. The logistic method is chosen because it is designed to predict the probability of a binary outcome, which is just the case for high pollution days (true or false). Since we find that the occurrences of extreme air pollution meteorology in previous

days also affect the high pollution episodes, both the extreme events in target day and the day before target day are taken as independent variables in the models.

We define the process of this prediction as HTA method, which is the combination of initial letters of heat waves (HW), temperature inversions (TI), and atmospheric stagnation episodes (AS). The governing equations for the prediction are

$$p(high) = \frac{1}{1 + e^{-t}} \tag{3.1}$$

$$t = b + t_{today} + t_{yesterday} \tag{3.2}$$

$$t_{today} = k_{HW_{today}} HW_{today} + k_{TI_{today}} TI_{today} + k_{AS_{today}} AS_{today} \tag{3.3}$$

where $p(high)$ is the probability of high pollution days; HW, TI and AS are the binary value shown the occurrences of heat waves, temperature inversions, and atmospheric stagnation episodes, respectively; t_{today} and $t_{yesterday}$ contain input data and coefficients for the target day (today) and the day before target day (yesterday), respectively; the equation of $t_{yesterday}$ is similar to Equation 3.3 with all the subscripts of *today* replaced by *yesterday*; b and k are the coefficients.

Since the emission level affects the relationship between extreme events and air quality, we detrend the concentrations of air pollutants in the study period before judge

the high pollution episodes, and only five previous years are used to derive the regression equations. To avoid the impacts of seasonal variability, we calculate the coefficients of regression model (b and k in Equation 3.2 and 3.3) with 91 running days around the target day, which are 45 days before and after the target day. When the sample size is less than 300 valid data points, the grid box is excluded.

For example, we try to predict whether 1 July 2013 is a high ozone day in a specific grid box. Ozone data are detrended for 1990-2015 period in this grid box. Then high ozone episodes are defined by judging top 10% most polluted days. The logistic model is built by calculating coefficients based on meteorological data and air pollution data from 17 May to 15 August in each year during 2008-2012. Once the coefficients (b and k) are found, we substitute the occurrences of extreme air pollution meteorology on 1 July 2013 in the regression model to get a prediction result. In the end, the status of high ozone day based on observational dataset is used to validate the prediction result.

We also introduce fire events into the prediction system. We first check the occurrences of fire events during 2001-2015. Then we compare the concentrations of air pollutants when fire happened (fire group) and when fire not happened (no fire group) to examine the importance of fire events to the formation of air pollutants. At last, we include fire as a predictor variables along with heat waves, temperature inversions,

and atmospheric stagnation episodes, and name it as HTA-fire method.

$$p(high) = \frac{1}{1 + e^{-f}} \tag{3.4}$$

$$f = b + f_{today} + f_{yesterday} \tag{3.5}$$

$$f_{today} = k_{HW_{today}} HW_{today} + k_{TI_{today}} TI_{today} + k_{AS_{today}} AS_{today} + k_{fire_{today}} fire_{today} \tag{3.6}$$

where fire is the occurrences of fire event on a given day in a given grid box. The comparison of HTA and HTA-fire methods reflect the relative importance of fire event in the development of high pollution episodes.

3.4 Results

We first investigate the cumulative effects of extreme air pollution meteorological events on high pollution episodes to figure out if we need to consider the status of extreme events in two consecutive days in regression models. If the target day is called today, or day 0, then the day before the target day can be called yesterday, or day -1. Similarly, two days before the target day can be called the day before yesterday, or day -2. We test the relationship between the occurrences of extreme air pollution meteorological events on previous days and the concentrations of air pollutants on the target day. We divide concentrations of a specific air pollutant on the target day

into two groups based on if a specific type of extreme air pollution methodological events occurred on day n, as shown in Equation 3.7.

$$PC = \frac{C_{event_{day\ n}} - C_{no_{day\ n}}}{C_{no_{day\ n}}} \times 100\% \tag{3.7}$$

where PC represents the percentage change in %; C represents that we are testing the concentration on the target day; *day n* represents that we divide all data points by considering the occurrences of a specific extreme air pollution meteorological event on the n*th* day, where n can be 0, -1, or -2; *event* is the group with that specific extreme air pollution meteorological event happened; *no* is the group without that specific extreme air pollution meteorological event happened. When the percentage change is positive, the concentration of air pollutant on the target day is elevated by the occurrences of extreme air pollution meteorological events on the n*th* day, and vice versa.

The test of the cumulative effects of extreme air pollution meteorological events (Table 3.1) indicates that the events happened before the target day also affect the concentrations of air pollutants on the target day. Although the amount of the elevated concentration is higher when the target day was a event day than when previous days were event days, we usually find the concentrations of ozone and $PM_{2.5}$ can also be elevated by the event happened before the target day. Exceptions are found in cases

of heat waves vs. $PM_{2.5}$, which may reflect the different responses of different components of $PM_{2.5}$ to heat waves. Since the day before the target day also affects the concentrations of the target day, we consider the status of extreme air pollution meteorological events in two consecutive days (Equation 3.1-3.3) as independent variables to make the prediction.

Table 3.1
Percentage change (%) of the concentration on the target day between the group with a specific extreme air pollution meteorological event on the n*th* day and the group without that event happened on the same day. * indicates statistically non-significant results at the 95% confidence interval.

Species	Season	Extreme events	Day 0	Day -1	Day -2
O_3	Summer	Heat wave	21.19	7.69	5.31
		Inversion	13.49	2.10	0.46
		Stagnation	12.77	4.64	3.06
$PM_{2.5}$	Summer	Heat wave	16.34	-1.03*	-6.67
		Inversion	29.21	15.06	10.54
		Stagnation	12.75	6.33	2.24
	Winter	Heat wave	0.19*	-14.74	-13.82
		Inversion	20.25	4.10	0.17*
		Stagnation	38.29	6.88	2.29

The prediction of high ozone days in 1995-2015 summer (June-August) with HTA method (Figure 3.1) shows similar magnitude and trend with AQS data, especially in the eastern United States. However, the interannual variation of high ozone days predicted by HTA method is not as strong as the one from AQS, which reflects that

although the extreme event is an important factor causing high ozone days, it is not the only factor that affects the frequency of high ozone days. We apply the correlation (R) between the time series of prediction results (HTA) and the time series of observational results (AQS) to validate the accuracy of our regression model. Overall, the correlation for the whole US domain is 0.77. For northeast region, the correlation between AQS and HTA results is 0.90, which implies that the changes of extreme events account for more than 80% of the interannual variations in high ozone pollution episodes in this region. The southeast region also has relatively high correlation between prediction result (HTA) and observational result (AQS), which is 0.75. All the western regions, including northwest, midwest, and southwest, show lower correlations, which are around 0.65.

The spatial distribution of correlations (Figure 3.2) reveals more detailed information. A large area in eastern regions and a small region of west coast have high correlations ranging from 0.6 to 0.9. However, the correlations in most western regions are much lower than eastern regions. A reason is our logistic regression model cannot be used in part of western regions where data are too few to reach a statistically significant level. Another potential reason of lower correlations in western regions might be the extreme low occurrences of temperature inversions and the stratospheric ozone intrusion.

The high $PM_{2.5}$ days are predicted for both summer (June-August) and winter

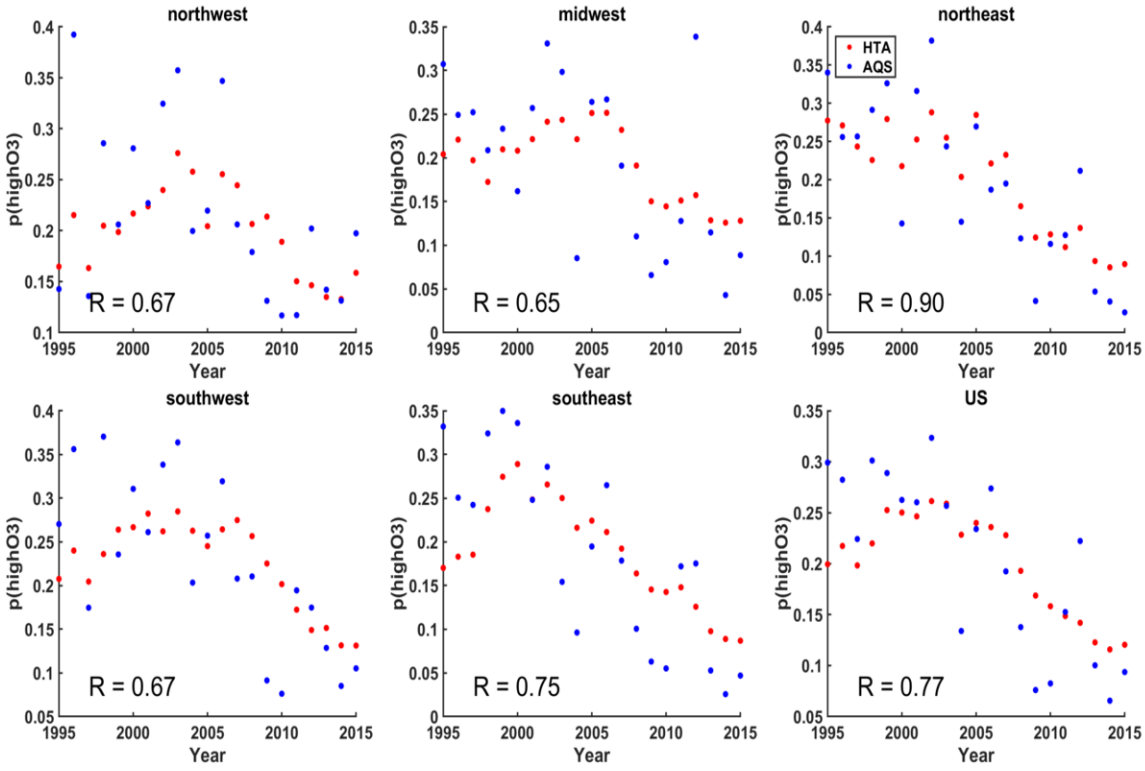

Figure 3.1: Compare the prediction of high ozone days (HTA) with the observed high ozone days (AQS) during summer in 1995-2015.

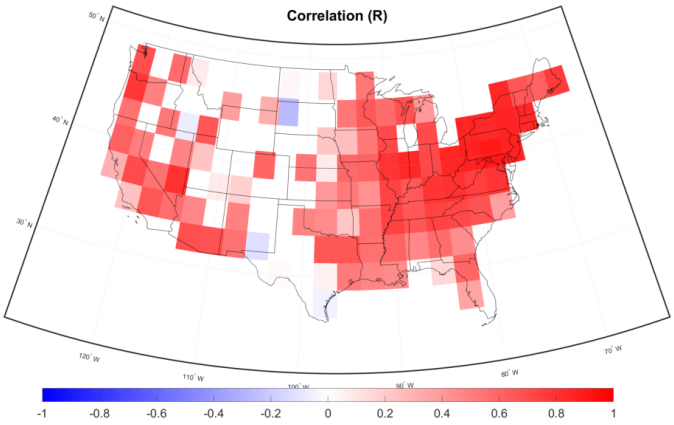

Figure 3.2: The correlation of the probability of high ozone days between AQS and HTA in 1996-2015 summer.

(December-February) during 2003-2015. Generally, the predictions of high $PM_{2.5}$ days in summertime (Figure 3.3) have lower correlations with observational results (AQS) when compared with the ozone case. The correlation is 0.69 for summer in the whole US and it varies in different regions. For example, the correlation is 0.87 in the northeast, and 0.63 in southeast. However, the correlations of all the western regions are only around 0.4. The reasons of relatively lower correlations in $PM_{2.5}$ cases are complex. One of the main reasons is the complicated components of $PM_{2.5}$. Different components respond differently to different types of extreme air pollution meteorological events. Another reason is that, when compare with ozone, there are less data points available for $PM_{2.5}$ in each year, and less years available. The lower correlation also implies the possibility of missing factors that are important for the high $PM_{2.5}$ episodes.

In winter, the correlations between the predicted high $PM_{2.5}$ episodes from HTA model and the observational results from AQS are even lower (Figure 3.4). For the whole US, the correlation is 0.43. The low accuracy of prediction in winter might be driven by the abated $PM_{2.5}$ in heat waves during winter. In a regional scale, southwest region has the highest correlation (0.77) between HTA result and AQS result, and northeast region has the lowest correlation (0.34). The spatial distribution of correlations in winter is significant different from what we see in summer. It reflects the seasonal change of main components of $PM_{2.5}$ and the changes of mechanisms about how extreme air pollution meteorological events affect air pollutants.

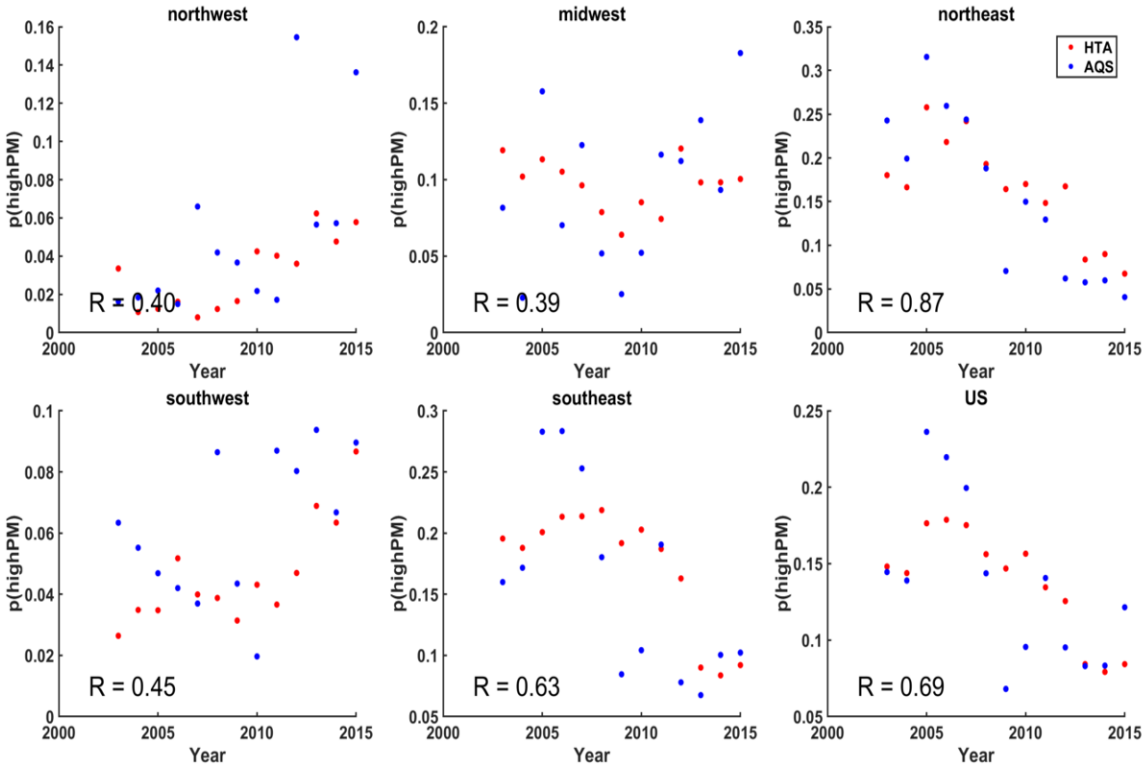

Figure 3.3: Compare the prediction of high PM days (HTA) with the observed high PM days (AQS) during summer in 2003-2015.

The correlations between the predicted high pollution episodes (HTA) and the observational high pollution episodes (AQS) give us a general idea about the performance of the HTA prediction. However, it only reflects the performance of interannual variability based on seasonal average. Since we aim to predict the occurrence of high pollution episode in each day, area under the receiver operating characteristic (AUROC) would be a good index to summarize the prediction accuracy of daily prediction. If the prediction is perfect, the value of AUROC would be 1; if all of the prediction results are random, the value of AUROC would be 0.5. We follow the criterion used by *Lee et al.* [2010] as shown in Table 3.2.

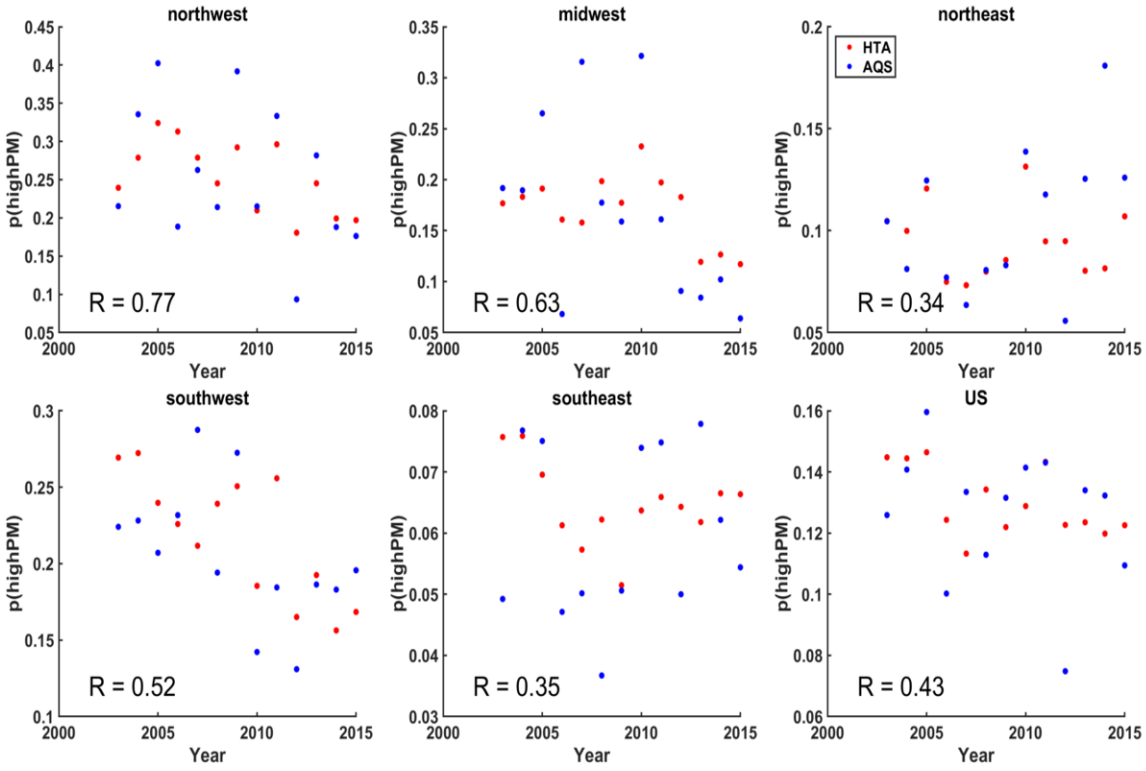

Figure 3.4: Compare the prediction of high PM days (HTA) with the observed high PM days (AQS) during winter in 2003-2015.

Table 3.2
AUROC criterion *Lee et al.* [2010].

AUROC range	Prediction performance
$AUROC < 0.6$	Poor
$0.6 \leqslant AUROC < 0.7$	Reasonable
$0.7 \leqslant AUROC < 0.8$	Good

Table 3.3 shows that most of our tests have reasonable predictions for each day's occurrences of high pollution episodes. The results agree with the correlations. In summer, our predictions perform best in the eastern US and bad in the western US.

And in winter, the performances are good in the western US. The bad performance in the western US in summer may reflect some missing factors that affect high pollution episodes in this region. Considering the strong effect of wildfire emission on air quality, we make the hypothesis that fire might be one of these dominant factors. So we further analyze fire events and add fir as the fourth independent variable in the regression models.

Table 3.3
AUROC of the HTA prediction validated by the AQS observational results. The normal font shows the reasonable prediction, the italic font shows the poor prediction, and the bold font shows the good prediction.

	Ozone	$PM_{2.5}$	
	1996-2015	2003-2015	
	Summer	Summer	Winter
Northwest	0.68	*0.57*	**0.73**
Midwest	0.66	0.60	0.63
Northeast	**0.79**	**0.72**	0.63
Southwest	0.60	*0.58*	**0.73**
Southeast	**0.70**	0.60	0.67
US	0.68	0.61	0.68

To examine the impact of fire events on air pollution, we first check the occurrences of fire events in 2001-2010 (Figure 3.5). The occurrences of fire events show large seasonal and spatial variations in US. Most fire events occur in summertime and are mainly located in the arid western US. Next, we investigate how the fire events affect the concentrations of ozone and $PM_{2.5}$ in 2001-2010 period based on the GFED4 data

and AQS data (Figure 3.6 and 3.7). The ratio of concentrations between fire group and no-fire group is used to study the enhancement of air pollution when fire occurs.

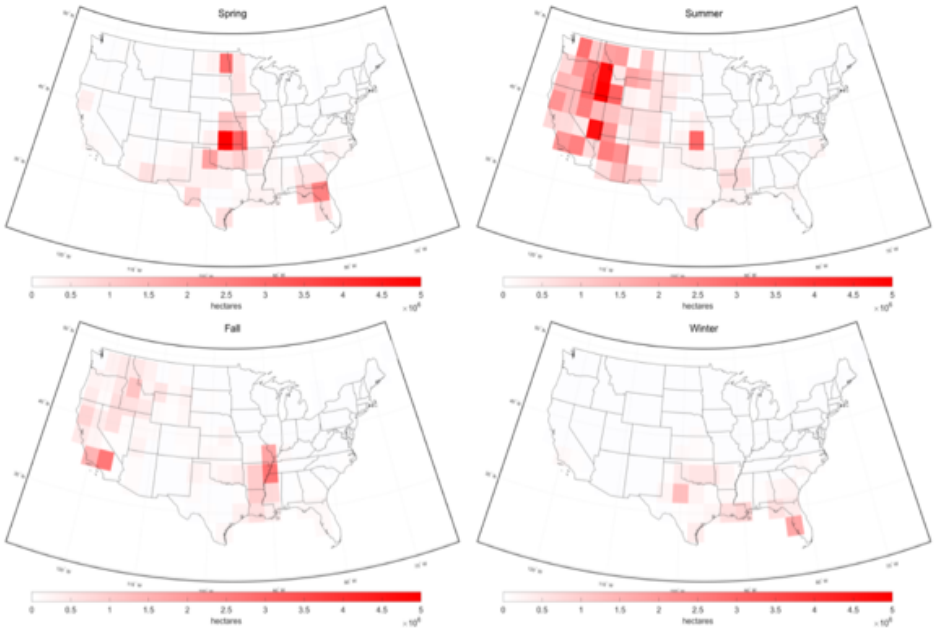

Figure 3.5: The average daily burned area (without small fires) in the unit of hectares during 2001-2010 period based on GFED4 dataset.

In general, ozone concentrations are higher in fire group (Figure 3.6). The reason might be that more ozone precursors are emitted through biomass burning in wildfire. The enhancement is stronger in fall and winter than summer time. This seasonal variation is driven by multiple potential factors. Firstly, the reduction of solar radiation due to high aerosol optical depths may reduce the photolysis rate and thus slow down the production of ozone in summer. Figure 3.7 supports this hypothesis that fire enhances the concentration of aerosols in the western US in summer, which is higher than the enhancement in other seasons. Secondly, ozone precursor is relatively

sufficient in summertime, so further increase of the ozone precursor is not as productive as the case with insufficient ozone precursors in other seasons. Thirdly, the pollutants from fire plume might inject into free troposphere and make long-range transportation that affects non-local regions instead. Last but not the least, even the absolute changes are the same in all seasons, the percentage change in summer would be lower than other seasons, because the average concentration of ozone is much higher in summer than other seasons.

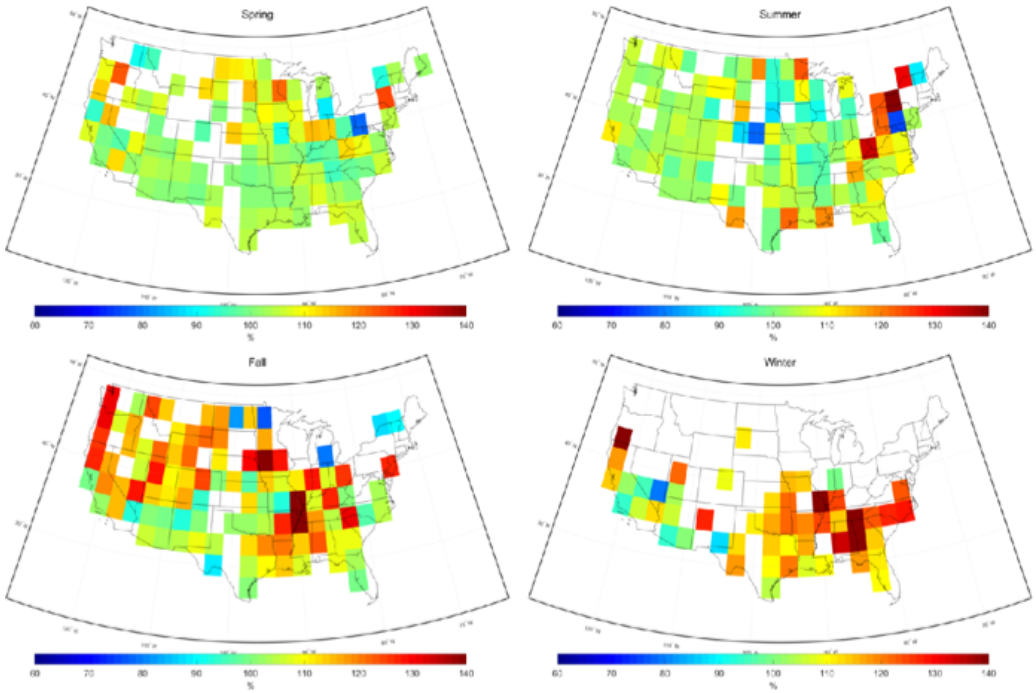

Figure 3.6: Enhancements in the seasonal average ozone concentrations by fire events during 2001-2010 period, shown as the ratio of mean concentrations on days with fire compared to those on days without fire. Blank regions indicate those with less than 3 data points for either group.

The concentrations of $PM_{2.5}$ are also enhanced by fire events (Figure 3.7), especially

in summer time. In fall and winter, the concentrations of $PM_{2.5}$ are lower in the western regions when fire events occur. This might be due to the differences in the main components of $PM_{2.5}$ in different seasons as discussed above.

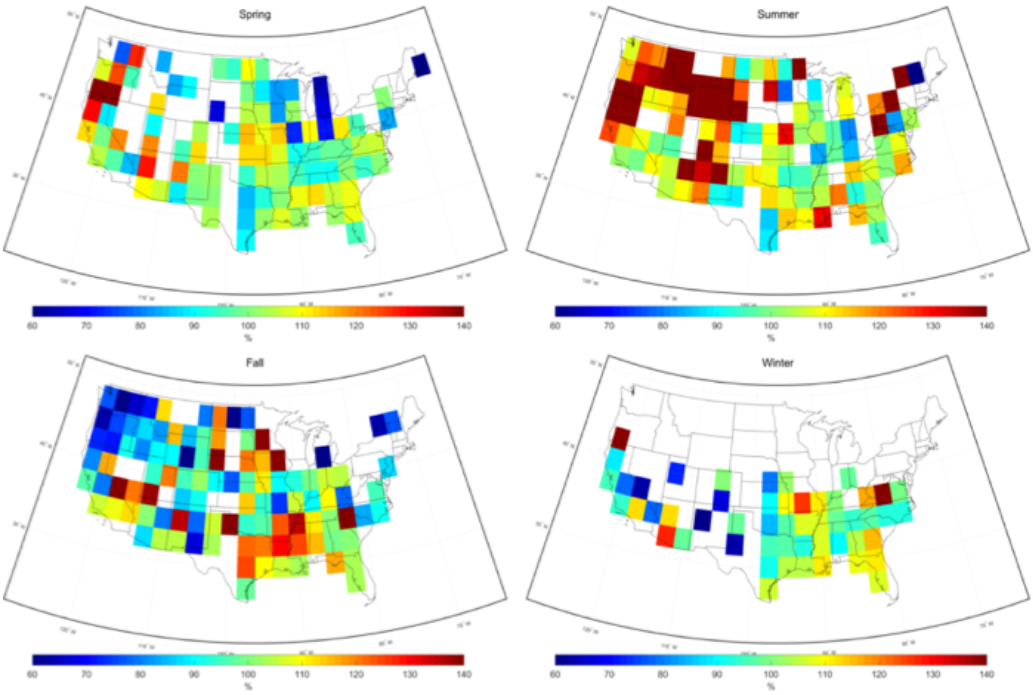

Figure 3.7: Enhancements in the seasonal average $PM_{2.5}$ concentrations by fire events during 2001-2010 period, shown as the ratio of mean concentrations on days with fire compared to those on days without fire. Blank regions indicate those with less than 3 data points for either group.

We include fire as the fourth variable in the logistic regression model to predict the high pollution days, which is named as HTA-fire method hereafter. We apply our model in the summer of 2006-2015 since fire happens mostly in summer. We calculate the correlation between the prediction results from HTA-fire and observational results from AQS, and check whether the value is higher than the correlation between HTA

and AQS. The percentage change between HTA and HTA-fire (Table 3.4) reflects the improvement of prediction when fire is considered in the method. The improvement of correlation is mainly found in northwest, where the correlation for ozone is increased by 27% and the correlation of $PM_{2.5}$ is increased by 105%. For this region, our results suggest that HTA-fire method is advisable to predict the probability of high pollution days compared with HTA method, which probably due to stronger emissions from fire. As shown in Figure 3.5, the occurrences of fire in summer in the western region are more than those in the eastern region. However, burned area and emission factors are also important factors associated with the concentrations of $PM_{2.5}$ other than fire count [*Clark et al.*, 2010; *Pearce et al.*, 2012; *Robertson et al.*, 2014; *Urbanski*, 2013]. So the different enhancement of $PM_{2.5}$ in northwest and southwest may be related to the higher fuel consumption in northwest than southwest [*Van der Werf et al.*, 2010]. Therefore, fire is an important factor for air quality in northwest region, which should be considered in the regression model. The limited improvement in other regions may related to the missing of small fires in our chosen fire database. GFED4 burned area without small fires is applied in this analysis due to the lack of high temporal resolution data in database with small fires. However, the small fires were found to be an important factor that increase the emission [*Randerson et al.*, 2012; *Zhang and Wang*, 2016]. So further analysis based on dataset that includes small fires is needed.

Another potential problem related to HTA-fire method is the prediction of fire events.

To predict the high pollution episodes with HTA-fire method in a near future, the predictions of heat waves, temperature inversions, atmospheric stagnation, and fire are needed. We can get reasonable predictions of other extreme air pollution meteorological events from weather forecast models, but it's hard to get reliable predictions of fire events. One main reason is lots of fires are human-ignited that are hard to be predicted by models. Even considering only the wildfires, there are still uncertainty related to the fire prediction models which further developments are needed [*Hantson et al.*, 2016]. In that case, our HTA-fire method would give out several potential probability of high pollution episodes for different cases of fire events.

Table 3.4
Percentage changes in the correlation between HTA-fire and AQS and the correlation between HTA and AQS during 2006-2015 summer.

Percentage Change	Ozone	$PM_{2.5}$
northwest	27.45%	104.64%
midwest	1.09%	−8.87%
northeast	0.00%	0.07%
southwest	8.31%	−0.35%
southeast	2.71%	−0.35%
US	5.52%	−0.40%

3.5 Conclusion

In this study, we build a series of logistic regression models to predict high pollution episodes with the occurrences of extreme air pollution meteorology around 2000s. By comparing the prediction results from our statistical models with the observational results from AQS dataset, we assess the accuracy of the prediction models. The correlation between the high pollution probability from statistical model and observational dataset and AUROC are applied as indexes to estimate the performance of our prediction. A high correlation suggests that 1) strong relationship between prediction results and observational results and 2) similar trends and interannual variations in both time series, while a high AUROC summarizes the performance of predictions in each day.

We discover large seasonal and spatial variations in most predictions. The prediction of high ozone episodes with heat waves, temperature inversions, and atmospheric stagnation episodes (HTA model) performs good in 1996-2015 summer. The correlation of the whole US is 0.77. Moreover, the correlation of northeast reaches 0.9, which means that more than 80% of the interannual variation in high ozone pollution episodes in this region is related to the occurrences of extreme air pollution meteorological events. The predictions of $PM_{2.5}$ are not as good as the ozone case, the correlation of the whole US are 0.69 and 0.43 for summer and winter, respectively,

which may be related to the complicated responses of the different components of $PM_{2.5}$ to different extreme air pollution meteorological events. The tests of AUROC generally agree with the tests of correlation.

We also analyze the relationship between fire and the concentrations of air pollutants. When fire happens, the ozone concentrations generally increase all over the US in all seasons. The increase is much stronger in fall and winter. For the concentrations of $PM_{2.5}$, the strongest increase by fire is in summer in western US. We introduce the fire events as an extra independent variable in our prediction model as HTA-fire model. The HTA-fire model increases the correlation of HTA by 27% for ozone and 105% for $PM_{2.5}$ in northwest region in summer.

The regression models give us further understanding about the relationships between high pollution episodes and multiple extreme air pollution meteorological events. In addition, we hope these statistical models can be used as a simple tool to provide the warnings of the high pollution episodes to the public with only simple information of upcoming extreme air pollution meteorology. The tool is especially reliable in northeast US for the prediction of high ozone days in summer.

Chapter 4

Sensitivity of Atmospheric Aerosol Scavenging to Precipitation Intensity and Frequency in the context of Global Climate Change

The material contained in this chapter has been submitted to *Atmospheric Chemistry and Physics* and has been published in *Atmospheric Chemistry and Physics Discussion*. Hou, P., S. Wu, and J. L. McCarty (2018), Sensitivity of atmospheric aerosol scavenging to precipitation intensity and frequency in the context of global climate change, *Atmospheric Chemistry and Physics*, in review.

4.1 Abstract

Wet deposition driven by precipitation is an important sink for atmospheric aerosols and soluble gases. We investigate the sensitivity of atmospheric aerosol lifetimes to precipitation intensity and frequency in the context of global climate change. Our sensitivity model simulations, through some simplified perturbations to precipitation in the GEOS-Chem model, show that the removal efficiency and hence the atmospheric lifetime of aerosols have significantly higher sensitivities to precipitation frequencies than to precipitation intensities, indicating that the same amount of precipitation may lead to different removal efficiencies of atmospheric aerosols. Combining the long-term trends of precipitation patterns for various regions with the sensitivities of atmospheric aerosol lifetimes to various precipitation characteristics allows us to examine the potential impacts of precipitation changes on atmospheric aerosols. Analyses based on an observational dataset show that precipitation frequencies in some regions have decreased in the past 14 years, which might increase the atmospheric aerosol lifetimes in those regions. Similar analyses based on multiple reanalysis meteorological datasets indicate that the changes of precipitation intensity and frequency over the past 30 years can lead to perturbations in the atmospheric aerosol lifetimes by 10% or higher at the regional scale.

4.2 Introduction

Wet scavenging is a major removal process for aerosols and soluble trace gases [*Atlas and Giam*, 1988; *Radke et al.*, 1980]. Global climate change implies significant perturbations of precipitation, which can directly affect the wet scavenging process. *Salzmann* [2016] found that the global mean precipitation did not change significantly since 1850 with climate models, while *Trenberth et al.* [2007] reported that the total precipitation amount increased over land north of 30N in the past century and decreased in the tropical region after the 1970s based on observational data. *Trenberth* [2011] also noted that theoretically a warmer climate could lead to less frequent but more intense precipitation.

The impacts of long-term changes in precipitation characteristics on air quality have not been well studied. Most previous studies focused on the correlation between air pollution and the total precipitation amount or precipitation intensity [*Cape et al.*, 2012; *Pye et al.*, 2009; *Tai et al.*, 2012]. For example, *Dawson et al.* [2007a] found a strong sensitivity of the $PM_{2.5}$ (particulate matters with diameters less than 2.5 μm) concentrations to precipitation intensity over a large domain of the eastern US with perturbation tests. Only a few studies focused on precipitation frequency. *Jacob and Winner* [2009] noted that precipitation frequency could be more important than

precipitation intensity for air quality because the wet scavenging process due to precipitation is very efficient [*Balkanski et al.*, 1993]. *Fang et al.* [2011] projected with the Geophysical Fluid Dynamics Laboratory chemistry-climate model (AM3) that wet deposition has a stronger spatial correlation with precipitation frequency than intensity over the US in January, although they concluded that frequency has a minor effect on wet deposition in the context of climate change. *Mahowald et al.* [2011] also discussed the importance of precipitation frequency in wet deposition based on simulations showing large removal rate of dust in precipitation events.

In this study, we first use GEOS-Chem, a global 3-D chemical transport model (CTM), to examine the sensitivities of atmospheric aerosol lifetimes to various precipitation characteristics, including the precipitation intensity, frequency, and total amount. By isolating these precipitation characteristics from other meteorological fields through a suite of perturbation simulations, we are able to better understand the sensitivities of atmospheric aerosols to various precipitation characteristics. We focus on black carbon (BC) as a proxy for atmospheric aerosols to examine the impacts of changes in precipitation characteristics. BC is nearly inert in the atmosphere [*Ramanathan and Carmichael*, 2008], making it a good tracer for studying the transport and deposition of atmospheric species. We also analyze the long-term trends of the precipitation characteristics over various regions around the world, based on the observational and reanalysis meteorological datasets for the past decades. We then combine the long-term trends in the precipitation patterns for various regions

with the sensitivities of BC to precipitation characteristics to quantify their potential impacts on atmospheric aerosols in the context of global climate change.

4.3 Methods

We utilize a global 3-D chemical transport model (CTM), GEOS-Chem version 9-02-01 [*Bey et al.*, 2001] (www.geos-chem.org), to carry out a suite of perturbation tests to examine the sensitivities of atmospheric aerosols to precipitation characteristics. As a chemical transport model, the GEOS-Chem model does not simulate meteorology prognostically; instead, it is driven by assimilated meteorological data from the Goddard Earth Observing System (GEOS) of NASA GMAO. We use the GEOS-5 meteorological dataset in this study. We conduct global simulations with a horizontal resolution of 4° latitude by 5° longitude and 47 vertical layers. All the model simulations in this study run from 1 July 2005 to 1 January 2007, i.e., for one and half years, with the first half year serving as the model spin-up.

The wet deposition scheme in GEOS-Chem includes scavenging in convective updrafts, in-cloud scavenging (rainout), and below-cloud scavenging (washout), which were described in detail by *Liu et al.* [2001] and *Wang et al.* [2011]. In GEOS-Chem simulation, the BC aerosols are classified into two types based on their hygroscopicity (hydrophobic vs. hydrophilic), and wet scavenging is more efficient for hydrophilic

BC. GEOS-Chem assumes the ratio between hydrophobic and hydrophilic BC to be 4:1 in fresh emissions and hydrophobic BC converts to hydrophilic one with an e-folding lifetime of 1.15 days.

The washout rate constant (k) is affected by the particle size and the form of precipitation. For washout by rain with precipitation rate P (mmh^{-1}), $k = 1.1 \times 10^{-3} P^{0.61}$ for accumulation mode (aerosols with diameters between 0.04 μm and 2.5 μm) and $k = 0.92P^{0.79}$ for coarse mode (aerosols with diameter between 2.5 μm to 16 μm); for washout by snow with precipitation rate P, $k = 2.8 \times 10^{-2} P^{0.96}$ for accumulation mode and $k = 1.57P^{0.96}$ for coarse mode [*Feng*, 2007, 2009]. The coefficients for accumulation-mode are used in calculating k for fine particles including BC in GEOS-Chem.

Our study focuses on three precipitation characteristics: the precipitation intensity, frequency, and total amount. We define precipitation events as the data points with significant (we use precipitation rate more than 1 mm/day as the criterion in this study) precipitation. Precipitation intensity is the average precipitation rate on precipitation events, with a unit of mm/day. Precipitation frequency is the fraction of precipitation events during the study period (i.e., the probability of any given data points with more than 1 mm/day precipitation rate), which is dimensionless. Total precipitation amount is defined as the average amount of precipitation rate during the study period, with a unit of mm/day. Assuming that precipitation is negligible

on data points with no precipitation events, we would have

$$total\ precipitation\ amount\ \cong\ precipitation\ intensity\ \cdot\ precipitation\ frequency \tag{4.1}$$

For sensitivity tests focused on precipitation intensity, we scale the base GEOS-5 precipitation values from the control run by a uniform factor for each grid box. For the sensitivity tests focused on precipitation frequency, we use a stochastic function to turn off the precipitation at a given data point. For example, in a simulation where we reduce the precipitation frequency by 25%, for a data point (i, j, t), we modify the initial precipitation rate $P_0(i, j, t)$ to

$$P(i,j,t) = \begin{cases} P_0(i,j,t); & R(i,j,t) \geqslant 0.25 \\ 0; & R(i,j,t) < 0.25 \end{cases} \tag{4.2}$$

where R is a random function with a range of (0, 1). In this way, we decrease the precipitation frequency of each grid box to 75% of its base value across the whole study domain and keep the base spatiotemporal precipitation patterns over each specific region.

For convenience in identifying and describing all the sensitivity tests, we name them after their precipitation frequency and intensity scaling factors. For instance, the case f0.5i2 represents the simulation with half the base precipitation frequency and twice

the base precipitation intensity, while the case f1i1 indicates the control simulation with a base frequency and intensity. We carry out more than 20 sensitivity model simulations to cover various precipitation intensities and frequencies as shown in Table 4.1.

The abundance of atmospheric aerosols is determined by both the aerosol emission rates and their atmospheric residence times, i.e., their lifetimes. The average atmospheric lifetimes of aerosols are calculated as

$$lifetime = \frac{burden}{removal\ rate} \tag{4.3}$$

$$lifetime = \frac{burden}{dry\ deposition\ rate\ +\ wet\ deposition\ rate} \tag{4.4}$$

Therefore, more efficient wet scavenging would lead to shorter atmospheric aerosol lifetimes.

We then examine the long-term changes in precipitation characteristics for various regions around the world in past decades. We first analyze changes in the precipitation between two 7-yr periods (2008-2014 vs. 2001-2007) based on an observational dataset, the 3-Hour Realtime Tropical Rainfall Measuring Multi-Satellite Precipitation Analysis version 7 (TRMM3B42v7, short for TRMM,

Table 4.1
Series of sensitivity model simulations carried out in this study.

Model simulations	Objective	Case names
Constant precipitation frequency (Figure 4.1a)	To study the sensitivity of BC lifetime to precipitation intensity	f1i0.25, f1i0.5, f1i1, f1i2, and f1i4
Constant precipitation intensity (Figure 4.1b)	To study the sensitivity of BC lifetime to precipitation frequency	f0.1i1, f0.25i1, f0.5i1, f0.75i1, and f1i1
Constant precipitation amount (Figure 4.1c)	To compare the sensitivity of BC lifetime to precipitation intensity and precipitation frequency	f0.1i10, f0.25i4, f0.5i2, f0.75i1.33, and f1i1
Hygroscopicity of aerosols (100% vs. 20% BC in fresh emissions are assumed to be hydrophilic)	To examine the impacts on wet deposition from the parameterization on the hygroscopicity of aerosols	f1i1 and f0.75i1.33
Aerosol size (BC aerosols are assumed to be in coarse mode vs. accumulation mode)	To examine the impacts on wet scavenging from the parameterization on the size of aerosols	f1i1 and f0.75i1.33
Contour of BC lifetime (Figure 4.2, 4.4-4.6)	To plot BC lifetime as a function of the precipitation intensity and frequency	f0.25i0.5, f0.25i1, f0.25i1.33, f0.25i2, f0.25i4, f0.5i0.5, f0.5i1, f0.5i1.33, f0.5i2, f0.5i4, f0.75i0.5, f0.75i1, f0.75i1.33, f0.75i2, f0.75i4, f1i0.5, f1i1, f1i1.33, f1i2, and f1i4

https://pmm.nasa.gov/TRMM). TRMM (3B42v7) performances better than the previous version of satellite products (3B42v6), though there are still problems in detecting precipitation events with low precipitation rates [*Maggioni et al.*, 2016]. We

then examine three reanalysis datasets with longer temporal coverage (2001-2010 vs 1981-1990): the National Centers for Environmental Prediction (NCEP) reanalysis dataset [*Kalnay et al.*, 1996], the NCEP-DOE AMIP-II (NCEP2) reanalysis dataset [*Kanamitsu et al.*, 2002], and NASA's Modern-Era Retrospective analysis for Research and Applications (MERRA) dataset [*Rienecker et al.*, 2011]. These datasets have different resolutions and spatial coverage. TRMM only covers 60^oN-60^oS, while other datasets cover the whole globe. The resolutions ($^\circ$ longitude $\times$ $^\circ$ latitude $\times$ hour) for TRMM, NCEP, NCEP2, and MERRA are $0.25 \times 0.25 \times 3$, $2.5 \times 2.5 \times 6$, $2.5 \times 2.5 \times 6$, $2.5 \times 2 \times 1$, respectively. We regrid the TRMM dataset from 0.25x0.25 to 2.5x2.5 ($^\circ$lon $\times$ $^\circ$lat) to reduce the computational cost and the relative errors at small precipitation rates [*Gehne et al.*, 2016; *Huffman et al.*, 2007]. By combining the resulting sensitivities of BC lifetimes to precipitation characteristics with the results of the long-term trends in precipitation characteristics, we then estimate the impacts of long-term changes in precipitation characteristics on the atmospheric lifetime of BC.

4.4 Results

The global annual mean lifetime of BC is calculated at 5.29 days in our control simulation (Figure 4.1). This value is similar to the results of a previous study, which stated that the lifetime of BC would be around one week [*Ramanathan and*

Carmichael, 2008]. Our result also agrees with the lifetime of 5.8±1.8 days simulated by the GEOS-Chem model [*Park et al.*, 2005] and the 5.4 days result simulated by the ECHAM5-HAM model [*Stier et al.*, 2005]. For 13 models in AeroCom, the lifetimes of BC from anthropogenic fossil fuel and biofuel sources are simulated to be from 3.5 to 17.1 days, with 5.9 days as the median value [*Samset et al.*, 2014].

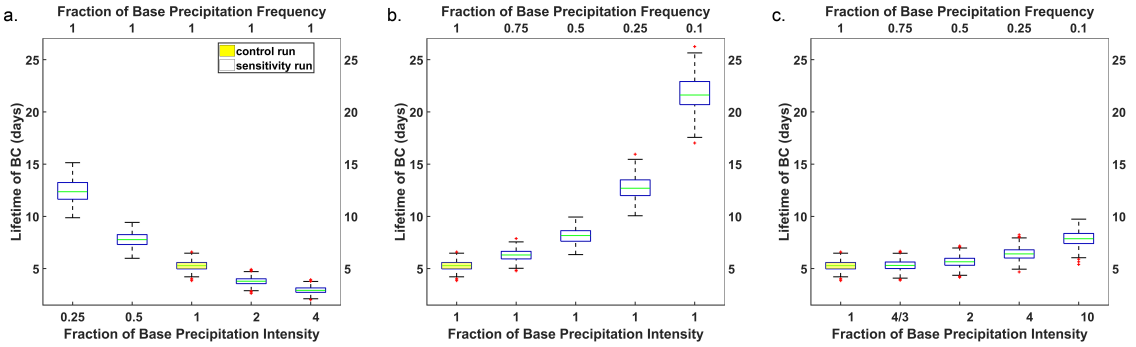

Figure 4.1: Impacts of the precipitation characteristics on the atmospheric lifetime of BC under given a) constant precipitation frequency; b) constant precipitation intensity; and c) constant precipitation amount. The top x-axis reflects the precipitation frequency set in each perturbation test, shown as fractions of base precipitation frequency. Base precipitation frequency is the precipitation frequency used in the control case. Similarly, the bottom x-axis reflects the settings of precipitation intensity in the perturbation tests. The box plot shows the probability distribution of BC lifetime for each case, where the top and bottom edges of each box show the third and first quartiles, respectively; the green central bar shows the median; the whisker shows the range of the non-outliers that cover 99.3% of the data, assuming normally distributed data; and the red plus shows the outliers.

We first compare the results of the control run with other simulations with the same precipitation frequency (f1i0.25, f1i0.5, f1i1, f1i2, and f1i4) to examine the sensitivity of BC lifetime to precipitation intensity (Figure 4.1a). We find that an increase in precipitation intensity leads to decreases in both the BC lifetime and the sensitivity

of the BC lifetime to precipitation intensity. That is, the impact of precipitation intensity on BC aerosols is saturated when the intensity is very high, which is consistent with a previous study [*Fang et al.*, 2011]. We then compare the control run with other simulations with the same precipitation intensity (f0.1i1, f0.25i1, f0.5i1, f0.75i1, and f1i1) to study the sensitivities of the BC lifetime to precipitation frequency (Figure 4.1b). Again, the BC lifetime responds non-linearly to the changes in precipitation frequency, and the sensitivity decreases with increases in precipitation frequency.

When we compare the simulations with a common precipitation amount (f0.1i10, f0.25i4, f0.5i2, f0.75i1.33, and f1i1), we find that the BC lifetime increases with increasing precipitation intensity (Figure 4.1c). For example, case f0.1i10 has an annual average BC lifetime of 7.86 days, which is much longer than the 5.29 days of the control simulation (case f1i1). This indicates that the sensitivity of the BC lifetime to precipitation frequency is stronger than that to the precipitation intensity.

The calculated efficiency of wet scavenging can be affected by model parameterizations. We first examine the possible impacts on our results from the parameterization on the hygroscopicity of aerosols. With the default parameterization in GEOS-Chem, 20% of the fresh BC emissions are assumed to be hydrophilic. We set up sensitivity runs with another parameterization, where all BC is assumed to be hydrophilic. With these two different parameterization schemes, we examine the changes in the BC lifetime between two scenarios (f1i1 vs. f0.75i1.33) respectively. We find that

with the default setting in GEOS-Chem, the atmospheric lifetime of BC under the f0.75i1.33 scenario is slightly higher than the f1i1 scenario by 0.4%. In comparison, if all the BC is assumed to be hydrophilic, the BC lifetime under the f0.75i1.33 scenario would be 3.6% higher. This implies that for hydrophilic aerosols, the sensitivity to precipitation frequency would be even higher.

We also evaluate the impacts on wet scavenging from aerosol size with sensitivity simulations. If we assume the aerosols to be in coarse mode, we find that it would lead to more efficient scavenging and consequently much shorter lifetime (compared to the default setting in GEOS-Chem that all BC aerosols are in accumulation mode). However, there are no significant effects on the relative sensitivities to precipitation frequency vs. intensity the percentage change in BC lifetime between the f1i1 and f0.75i1.33 scenarios is very similar to the cases with parameterization for accumulation mode (0.3% vs. 0.4%). This indicates that the relative sensitivity of the BC lifetime to precipitation frequency and precipitation intensity is not significantly affected by the parameterization of particle size in the wet scavenging scheme in GEOS-Chem. It is worth noting that our model does not resolve the size of precipitation droplet, which can also affect the efficiency of wet scavenging.

The stronger sensitivity of the BC lifetime to precipitation frequency than that to intensity implies that an increase in the total precipitation amount does not necessarily lead to a decrease in the BC lifetime. This is better illustrated in Figure 4.2, which

shows the BC lifetime as a function of the precipitation intensity and frequency based on 20 cases (f0.25, f0.5, f0.75, f1 versus i0.5, i1, i1.33, i2, i4). Compared with the control scenario (i.e., f1i1, the base precipitation intensity and frequency, as labeled by the black star), any point in the area between the two solid curves (the green one shows a constant total precipitation amount, and the red one shows a constant BC lifetime) would have a higher total precipitation amount and a longer BC lifetime. This indicates that, even with an increased total precipitation, the BC lifetime (and hence the atmospheric concentrations of BC) can still increase if the precipitation frequency decreases significantly. This feature may help explain the decrease of the wet deposition flux found in wetter future climate simulations, despite their slightly increased total precipitation amounts [*Xu et al.*, 2018].

The lifetime contour plot in Figure 4.2 can be employed as a simple tool to help us understand the impacts of long-term changes in precipitation on atmospheric aerosols, so we also investigate the long-term trends in the precipitation characteristics over the past decades for various regions around the world. In considering the spatial variations of precipitation patterns and their long-term trends, we divide the global continental regions into multiple subcontinental areas to better resolve the spatial variations (Figure 4.3). We first carry out an analysis based on precipitation data from the TRMM dataset. The changes in the average precipitation intensities and frequencies between the periods of 2008-2014 and 2001-2007 for each region are shown as ratios in Figure 4.4, with the width and height of the blocks in Figure 4.4 indicating the

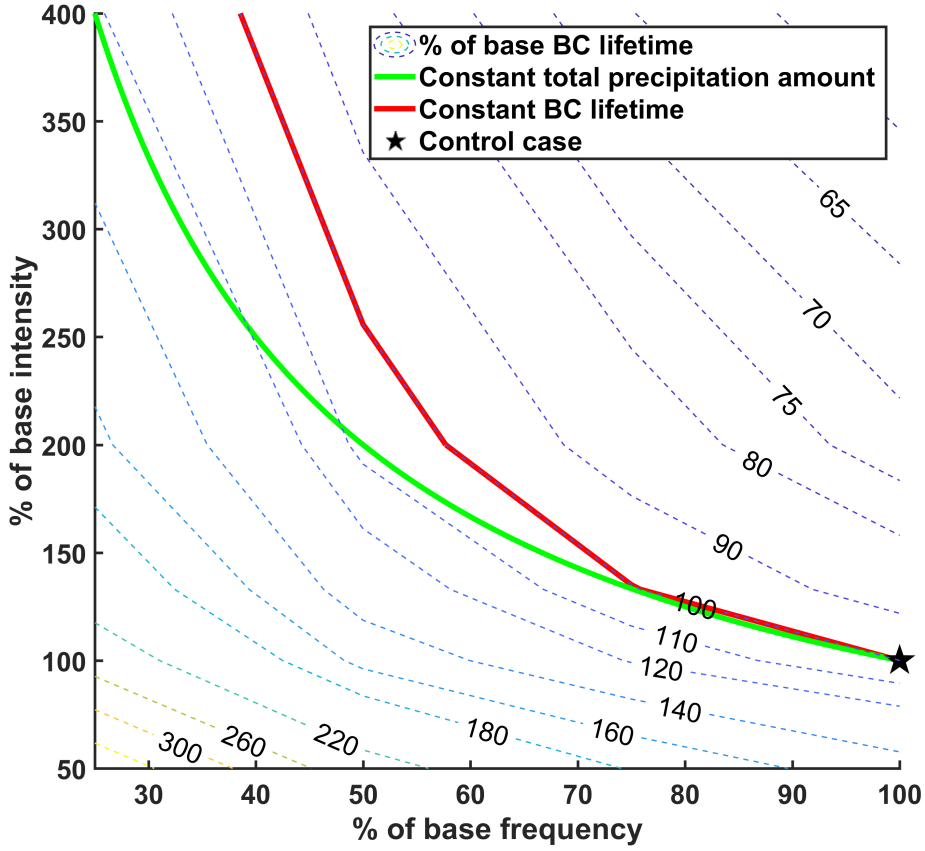

Figure 4.2: Model calculated BC atmospheric lifetime as a function of precipitation intensity and frequency. The dashed contour lines indicate the atmospheric lifetimes of the black carbon aerosols from the interpolation of 20 cases, which show the potential changes of BC lifetimes from the base BC lifetime (in the control run) driven by the changes of precipitation intensity and frequency. The green solid line represents a total precipitation equal to that of the base simulation (control run). The red solid line indicates the conditions leading to atmospheric black carbon aerosol lifetimes that match the base simulation (control run).

standard errors of the calculated percentage changes in precipitation frequency and intensity, respectively. Although these TRMM data only cover 14 years, the standard errors as shown in Figure 4.4 indicate that the changes in precipitation intensity and frequency over most regions are statistically significant. We find that during these

14 years, the average precipitation intensity has increased over most regions, but the average precipitation frequency has decreased over more than one third of the total regions including western North America (nwNA and swNA), southern South America (sSA), western Europe (wEU), southern Africa (sAF), and southwestern Asia (swAS). Based on the TRMM dataset, we find that almost all (5 out of 6) of the regions with decreasing precipitation frequency are expected to experience longer atmospheric aerosol lifetimes.

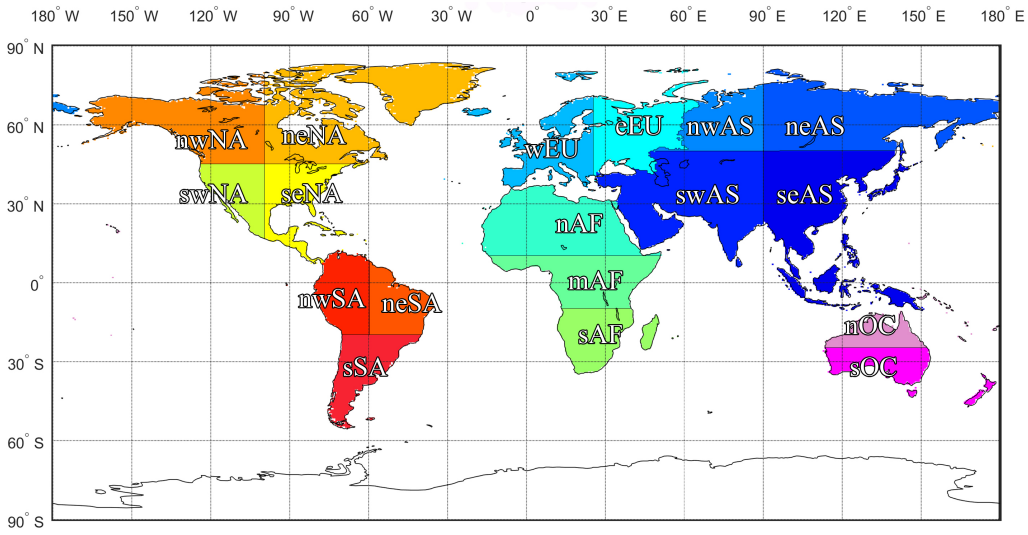

Figure 4.3: The definitions of the continental regions in this study. The uppercase letters in the region names represent the names of their continents: North America (NA), South America (SA), Europe (EU), Africa (AF), Asia (AS), and Oceania (OC). The lowercase letters in the region names represent the subregions inside the continent: north (n), south (s), west (w), east (e), middle (m), northwest (nw), northeast (ne), southwest (sw), and southeast (se).

Since the TRMM data only cover a relatively short period, we make similar analyses with three reanalysis datasets (NCEP, NCEP2, and MERRA) to cover a longer time period (2001-2010 vs. 1981-1990) (Figure 4.5). We find that, similar to the TRMM

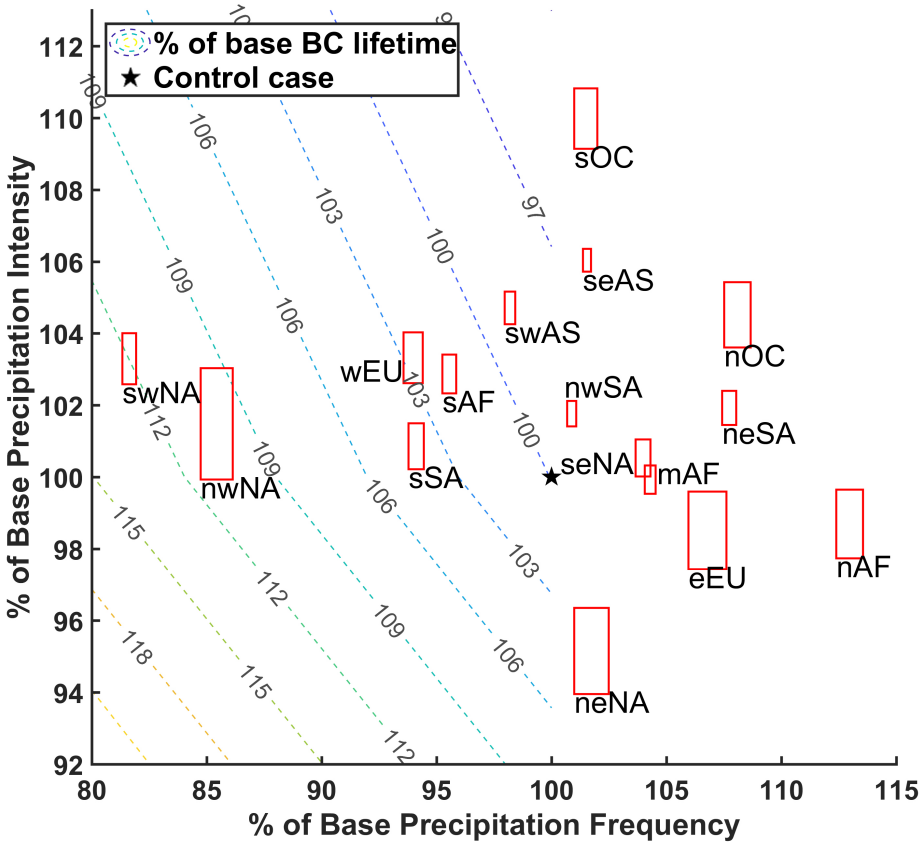

Figure 4.4: The potential change of atmospheric BC aerosol lifetime driven by the changes between the two periods (2008-2014 and 2001-2007) in precipitation characteristics based on meteorological datasets TRMM. The dashed contours are the same as in Fig. 2, which indicate the atmospheric lifetimes of the black carbon aerosols from the interpolation of 20 cases and show the potential changes of BC lifetimes from the base BC lifetime (in the control run) driven by the changes of precipitation intensity and frequency. Red blocks show the changes of precipitation intensities and frequencies, with the size of the block showing the standard error of the percentage changes.

data, all the three reanalysis datasets show increasing trends for precipitation intensity over most regions but more divergent trends for precipitation frequency in the past decades. The NCEP data show that precipitation frequency has decreased over about two-thirds of the total regions while NCEP2 and MERRA data show

decreasing precipitation frequency over one third and half of the total regions, respectively. In addition, even when the different datasets indicate the same direction for the precipitation change over a specific region, the magnitude of the changes may vary significantly across datasets. For example, the derived changes in the average precipitation intensity over neNA (northeastern North America) based on NCEP, NCEP2, and MERRA data are +8%, +12%, and +3% respectively. These variations across different data sources reflect the significant uncertainties associated with these datasets, as reported earlier [e.g. *Gehne et al.*, 2016; *Trenberth and Guillemot*, 1998; *Trenberth*, 2011].

On the other hand, previous analysis on global land-average precipitation showed that various reanalysis datasets have similar trends and interannual variability with other gauge- and satellite-based datasets during 2001-2010, though the estimated trend of precipitation varies based on temporal and spatial scales [*Gehne et al.*, 2016]. In addition, our study focuses on the changes over continental regions, where the precipitation data in the reanalysis datasets are found to be more reliable than over the ocean regions [*Trenberth*, 2011]. Therefore despite the uncertainties associated with each meteorological dataset, we can use Fig. 5 to estimate the expected changes in the atmospheric BC lifetimes for certain regions, especially for those regions showing consistent trends across different datasets. Assuming the effects of precipitation on wet deposition is the only factor that affects the atmospheric BC aerosol lifetimes, all three datasets indicate that atmospheric BC aerosol lifetimes could have decreased

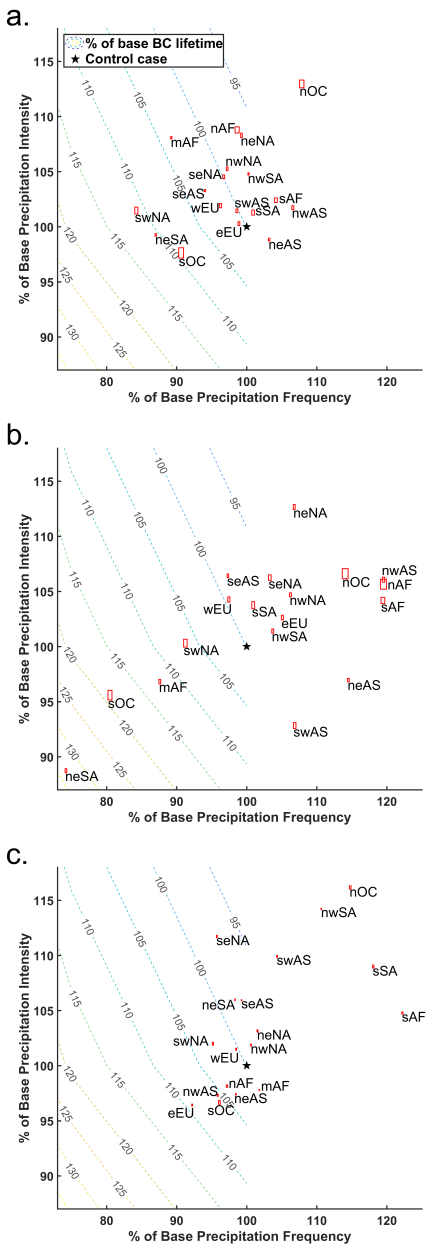

Figure 4.5: The potential change of atmospheric BC aerosol lifetime driven by the changes between the two periods (2001-2010 and 1981-1990) in precipitation characteristics based on multiple meteorological datasets: a). NCEP; b). NCEP2; c). MERRA. The dashed contours are the same as in Fig. 2, which indicate the atmospheric lifetimes of the black carbon aerosols from the interpolation of 20 cases and show the potential changes of BC lifetimes from the base BC lifetime (in the control run) driven by the changes of precipitation intensity and frequency. Red blocks show the changes of precipitation intensities and frequencies, with the size of the block showing the standard error of the percentage changes.

in the northern regions of North America (neNA and nwNA), the northwestern and southern regions of South America (nwSA and sSA), South Africa (sAF), and North Oceania (nOC). All three meteorological datasets show increasing trends in aerosol lifetimes over southwestern North America (swNA), Middle Africa (mAF), and South Oceania (sOC), which imply increasing trends for the concentrations of particulate matter ($PM_{2.5}$) over these regions, driven by changes in precipitation. At the regional scale, precipitation changes over the past 30 years can easily lead to perturbations in atmospheric BC lifetimes by 10% or higher.

We should note that there are some caveats for our idealized sensitivity simulations. The way we reduce precipitation frequency in the model (based on a stochastic function as discussed in Section 4.3) can be very different from climate-driven precipitation change in the real world. The globally uniform scaling factors applied to precipitation intensity do not account for the spatial variations. As a consequence, the sensitivities of BC lifetime to precipitation changes over a specific region may be different from those shown in Figure 4.2. To partly address this issue, we have constructed some regional contour plots similar to that in Figure 4.2 but based on sensitivities of BC lifetime for those specific regions (Figure 4.6). Comparison of these regional contours with the global one indicate some differences in the sensitivity of BC to precipitation changes, but generally less than 3

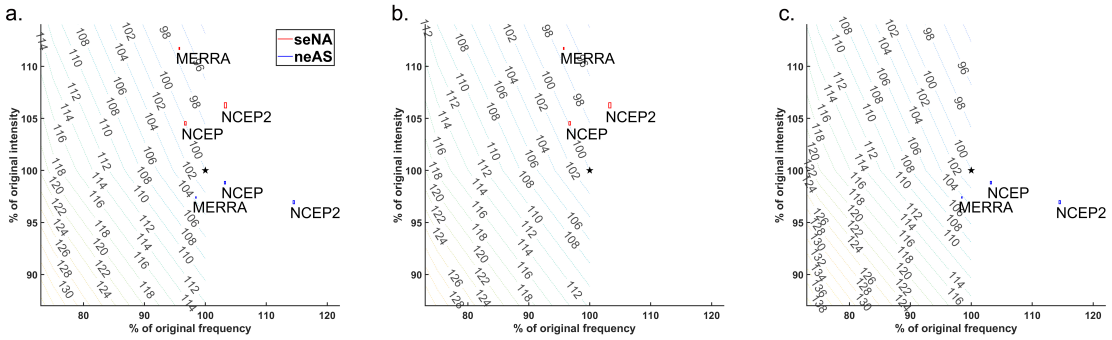

Figure 4.6: Compare the contours calculated on the global and regional scale: a). global; b). southeast North America (seNA); c). northeast Asia (neAS). The contours indicate the atmospheric lifetimes of the black carbon aerosols from the interpolation of 20 cases and show the potential changes of BC lifetimes from the base BC lifetime (in the control run) driven by the changes of precipitation intensity and frequency. The contour calculated on the global scale is the same with Figure 4.2. seNA and neAS are two most extreme cases among all regions, with the smallest and largest sensitivities between BC lifetimes and precipitation changes.

4.5 Conclusions and Discussion

The efficiency of the wet scavenging of atmospheric aerosols is affected by not only the precipitation amount but also the precipitation patterns. Our results, based on sensitivity simulations with the GEOS-Chem model, show that the atmospheric lifetimes of BC are more sensitive to precipitation frequency than precipitation intensity, and as a consequence, increases in the total precipitation amount do not always lead to a more efficient wet scavenging of atmospheric aerosols. The sensitivities of the atmospheric lifetimes of aerosols to the precipitation characteristics derived from our model simulations offer a simple and convenient tool for us to better examine the implications of long-term changes in precipitation (including the total amounts and

patterns) for atmospheric aerosols in various regions.

Analysis of satellite data (TRMM) for the past 14 years (2001-2014) reveals that precipitation intensity has increased in most regions. On the other hand, decreasing precipitation frequency are found in some regions such as western North America, southern South America, western Europe, southern Africa, and southwestern Asia. The decreases in precipitation frequency could lead to increases in atmospheric aerosol lifetimes over these regions. Our further analyses based on three meteorological datasets (NCEP, NCEP2, and MERRA) for the past decades (1981-2010) show increases in precipitation intensities over most continental regions, but significant decreases in precipitation frequency are identified over some regions. These changes in precipitation characteristics affect the wet deposition of aerosols and consequently the total burdens of aerosols and their atmospheric lifetimes. Despite the significant uncertainties associated with meteorological data, we find that the changes in precipitation intensity and frequency over the past 30 years could have led to perturbations in the regional atmospheric aerosol lifetimes by 10% or higher. Our results are consistent with *Kloster et al.* [2010] and *Fang et al.* [2011] that who reported increasing atmospheric aerosol burden due to climate change, although their results are based on future climate change. We also find that all three meteorological databases are consistent to show that the changes in precipitation intensity and frequency over the past decades have led to decreases in atmospheric aerosol lifetimes over the northern regions of North America, northwestern and southern regions of South America,

South Africa, and North Oceania. They are also consistent in indicating increasing trends of atmospheric aerosol lifetimes in the southwestern region of North America, Middle Africa, and South Oceania. The increasing trends in atmospheric aerosol lifetimes over these regions driven by the changes in precipitation intensity and frequency in the context of global climate change could pose challenges for the local PM air qualities. It should be noted that the results from this work can be affected by the parameterization in the GEOS-Chem model and have certain limitations. Our study does not account for the impacts of precipitation on wildfires which can emit a massive amount of aerosols including BC [*Dawson et al.*, 2014].

Chapter 5

Conclusion

My analyses on multiple meteorological databases reveal that the extreme air pollution meteorological events, such as heat waves, temperature inversions, and atmospheric stagnation episodes, have significantly increased globally in the past decades. To investigate the implications of these changes on air quality, I quantify the potential impacts of extreme air pollution meteorology on air quality in the 2000s based on both the observational data and the model simulation results. I find that both the averaged concentrations of air pollutants and the frequency of high pollution episodes increase when the extreme air pollution meteorological events happen in most seasons and regions over the United States.

I develop simple statistical tools, HTA and HTA-fire methods, to predict the high

air pollution episodes based on the relationships between extreme air pollution meteorological events and the air quality. These simple tools are more convenient than chemical transport model (CTM). They are useful when the CTM simulation is not available due to the lack of time or necessary input data, though the accuracy varies with species, seasons, and regions. More importantly, the prediction results reveal potential impacts of climate change on air quality due to the change of extreme air pollution meteorological events. These changes and the associated public health risk need to be considered in the long-term planning of air pollution control strategies by the environmental managers.

I study how the changes of precipitation patterns impact atmospheric aerosols. Results reveal that the atmospheric lifetimes of BC are more sensitive to precipitation frequency than precipitation intensity based on the sensitivity tests with GEOS-Chem model. In other words, when the precipitation frequency decreases, the increase of total precipitation amount may not lead to a more efficient wet scavenging of atmospheric aerosols. The relationship between the lifetimes of aerosols and the change of precipitation characteristics provides a simple tool (aerosol contours) to examine the impacts of long-term changes in precipitation intensity and precipitation frequency to atmospheric aerosols in various regions.

Based on my analysis, the increases of extreme air pollution meteorological events in

the context of climate change may risk public health and cause social and environmental issues. Although the concentrations of surface ozone decreased in a large area by the efforts of controlling anthropogenic emissions, such as the NO_x Statement Implementation Plan [*Frost et al.*, 2006], we have to prevent the climate penalty driven by the changes of extreme air pollution meteorology through establishing stricter environmental laws. More researches are needed to better understand the mechanisms and to solve the problems. I managed to exclude the effects of emissions by working on shorter time period and detrending. More work about how the emission affects the relationship between air pollutants and extreme air pollution meteorology would be necessary, which would be helpful in better quantifying the emission control considering the changes of extreme events in the far future.

References

Abdul-Wahab, S. A., C. S. Bakheit, and S. M. Al-Alawi (2005), Principal component and multiple regression analysis in modelling of ground-level ozone and factors affecting its concentrations, *Environmental Modelling & Software*, *20*(10), 1263–1271.

Alexander, B., and L. J. Mickley (2015), Paleo-perspectives on potential future changes in the oxidative capacity of the atmosphere due to climate change and anthropogenic emissions, *Current Pollution Reports*, *1*(2), 57–69.

Alexander, L. V., X. Zhang, T. C. Peterson, J. Caesar, B. Gleason, A. M. G. Klein Tank, M. Haylock, D. Collins, B. Trewin, F. Rahimzadeh, et al. (2006), Global observed changes in daily climate extremes of temperature and precipitation, *Journal of Geophysical Research: Atmospheres*, *111*(D5).

Atlas, E., and C. S. Giam (1988), Ambient concentration and precipitation scavenging of atmospheric organic pollutants, *Water, Air, & Soil Pollution*, *38*(1), 19–36.

Balachandran, S., K. Baumann, J. E. Pachon, J. A. Mulholland, and A. G. Russell (2017), Evaluation of fire weather forecasts using $PM_{2.5}$ sensitivity analysis, *Atmospheric Environment*, *148*, 128–138.

Balkanski, Y. J., D. J. Jacob, G. M. Gardner, W. C. Graustein, and K. K. Turekian (1993), Transport and residence times of tropospheric aerosols inferred from a global three-dimensional simulation of ^{210}Pb, *Journal of Geophysical Research: Atmospheres*, *98*(D11), 20,573–20,586.

Bey, I., D. J. Jacob, R. M. Yantosca, J. A. Logan, B. D. Field, A. M. Fiore, Q. Li, H. Y. Liu, L. J. Mickley, and M. G. Schultz (2001), Global modeling of tropospheric chemistry with assimilated meteorology: Model description and evaluation, *Journal of Geophysical Research: Atmospheres*, *106*(D19), 23,073–23,095.

Bloomer, B. J., J. W. Stehr, C. A. Piety, R. J. Salawitch, and R. R. Dickerson (2009), Observed relationships of ozone air pollution with temperature and emissions, *Geophysical Research Letters*, *36*(9).

Brunekreef, B., and S. T. Holgate (2002), Air pollution and health, *The lancet*, *360*(9341), 1233–1242.

Camalier, L., W. Cox, and P. Dolwick (2007), The effects of meteorology on ozone in urban areas and their use in assessing ozone trends, *Atmospheric Environment*, *41*(33), 7127–7137.

Cape, J. N., M. Coyle, and P. Dumitrean (2012), The atmospheric lifetime of black carbon, *Atmospheric environment*, *59*, 256–263.

Cardelino, C. A., and W. L. Chameides (1990), Natural hydrocarbons, urbanization, and urban ozone, *Journal of Geophysical Research: Atmospheres*, *95*(D9), 13,971–13,979.

Carmichael, G. R., I. Uno, M. J. Phadnis, Y. Zhang, and Y. Sunwoo (1998), Tropospheric ozone production and transport in the springtime in east Asia, *Journal of Geophysical Research: Atmospheres*, *103*(D9), 10,649–10,671.

CCSP (2008), *Weather and Climate Extremes in a Changing Climate. Regions of Focus: North America, Hawaii, Caribbean, and U.S. Pacific Islands.*, US Climate Change Science Program, Department of Commerce, NOAAs National Climatic Data Center, Washington, D.C., USA.

Chen, L.-W. A., J. G. Watson, J. C. Chow, M. C. Green, D. Inouye, and K. Dick (2012), Wintertime particulate pollution episodes in an urban valley of the Western US: a case study, *Atmospheric Chemistry and Physics*, *12*(21), 10,051–10,064.

Clark, K., N. Skowronski, G. Michael, W. E. Heilman, and J. Hom (2010), Fuel consumption and particulate emissions during fires in the New Jersey Pinelands.

Council, N. R., et al. (2008), *Estimating mortality risk reduction and economic benefits from controlling ozone air pollution*, National Academies Press.

Dawson, J. P., P. J. Adams, and S. N. Pandis (2007a), Sensitivity of $PM_{2.5}$ to climate in the Eastern US: a modeling case study, *Atmospheric chemistry and physics*, *7*(16), 4295–4309.

Dawson, J. P., P. J. Adams, and S. N. Pandis (2007b), Sensitivity of ozone to summertime climate in the eastern USA: A modeling case study, *Atmospheric environment*, *41*(7), 1494–1511.

Dawson, J. P., B. J. Bloomer, D. A. Winner, and C. P. Weaver (2014), Understanding the meteorological drivers of US particulate matter concentrations in a changing climate, *Bulletin of the American Meteorological Society*, *95*(4), 521–532.

Dentener, F., D. Stevenson, K. Ellingsen, T. van Noije, M. Schultz, M. Amann, C. Atherton, N. Bell, D. Bergmann, I. Bey, et al. (2006), The global atmospheric environment for the next generation, *Environmental Science & Technology*, *40*(11), 3586–3594.

D'Ippoliti, D., P. Michelozzi, C. Marino, F. De'Donato, B. Menne, K. Katsouyanni, U. Kirchmayer, A. Analitis, M. Medina-Ramón, A. Paldy, et al. (2010), The impact of heat waves on mortality in 9 European cities: results from the EuroHEAT project, *Environmental Health*, *9*(1), 37.

Doherty, R. M., O. Wild, D. T. Shindell, G. Zeng, I. A. MacKenzie, W. J. Collins, A. M. Fiore, D. S. Stevenson, F. J. Dentener, M. G. Schultz, et al. (2013), Impacts

of climate change on surface ozone and intercontinental ozone pollution: A multi-model study, *Journal of Geophysical Research: Atmospheres*, *118*(9), 3744–3763.

Easterling, D. R., G. A. Meehl, C. Parmesan, S. A. Changnon, T. R. Karl, and L. O. Mearns (2000), Climate extremes: observations, modeling, and impacts, *science*, *289*(5487), 2068–2074.

Emberson, L. D., D. Simpson, J. P. Tuovinen, M. R. Ashmore, and H. M. Cambridge (2000), Towards a model of ozone deposition and stomatal uptake over Europe, *EMEP MSC-W Note*, *6*(2000), 1–57.

Englert, N. (2004), Fine particles and human healtha review of epidemiological studies, *Toxicology letters*, *149*(1-3), 235–242.

Fang, Y., A. M. Fiore, L. W. Horowitz, A. Gnanadesikan, I. Held, G. Chen, G. Vecchi, and H. Levy (2011), The impacts of changing transport and precipitation on pollutant distributions in a future climate, *Journal of Geophysical Research: Atmospheres*, *116*(D18).

Feng, J. (2007), A 3-mode parameterization of below-cloud scavenging of aerosols for use in atmospheric dispersion models, *Atmospheric Environment*, *41*(32), 6808–6822.

Feng, J. (2009), A size-resolved model for below-cloud scavenging of aerosols by snowfall, *Journal of Geophysical Research: Atmospheres*, *114*(D8).

Fiala, J., L. Cernikovsky, F. de Leeuw, and P. Kurfuerst (2003), Air pollution by ozone in Europe in summer 2003, *Overview of exceedances of EC ozone threshold values during the summer season April–August*, p. 33.

Filleul, L., S. Cassadou, S. Médina, P. Fabres, A. Lefranc, D. Eilstein, A. Le Tertre, L. Pascal, B. Chardon, M. Blanchard, et al. (2006), The relation between temperature, ozone, and mortality in nine French cities during the heat wave of 2003, *Environmental health perspectives*, *114*(9), 1344.

Fiore, A., D. J. Jacob, H. Liu, R. M. Yantosca, T. D. Fairlie, and Q. Li (2003), Variability in surface ozone background over the United States: Implications for air quality policy, *Journal of Geophysical Research: Atmospheres*, *108*(D24).

Fiore, A. M., V. Naik, D. V. Spracklen, A. Steiner, N. Unger, M. Prather, D. Bergmann, P. J. Cameron-Smith, I. Cionni, W. J. Collins, et al. (2012), Global air quality and climate, *Chemical Society Reviews*, *41*(19), 6663–6683.

Fiore, A. M., V. Naik, and E. M. Leibensperger (2015), Air quality and climate connections, *Journal of the Air & Waste Management Association*, *65*(6), 645–685.

Francis, J. A., and S. J. Vavrus (2012), Evidence linking Arctic amplification to extreme weather in mid-latitudes, *Geophysical Research Letters*, *39*(6).

Frich, P., L. V. Alexander, P. Della-Marta, B. Gleason, M. Haylock, A. K. Tank,

and T. Peterson (2002), Observed coherent changes in climatic extremes during the second half of the twentieth century, *Climate research*, *19*(3), 193–212.

Frost, G. J., S. A. McKeen, M. Trainer, T. B. Ryerson, J. A. Neuman, J. M. Roberts, A. Swanson, J. S. Holloway, D. T. Sueper, T. Fortin, et al. (2006), Effects of changing power plant NOx emissions on ozone in the eastern United States: Proof of concept, *Journal of Geophysical Research: Atmospheres*, *111*(D12).

Gao, Y., J. S. Fu, J. B. Drake, J.-F. Lamarque, and Y. Liu (2013), The impact of emission and climate change on ozone in the United States under representative concentration pathways (RCPs), *Atmospheric Chemistry and Physics*, *13*(18), 9607–9621.

Gehne, M., T. M. Hamill, G. N. Kiladis, and K. E. Trenberth (2016), Comparison of global precipitation estimates across a range of temporal and spatial scales, *Journal of Climate*, *29*(21), 7773–7795.

Gupta, P., and S. A. Christopher (2009), Particulate matter air quality assessment using integrated surface, satellite, and meteorological products: Multiple regression approach, *Journal of Geophysical Research: Atmospheres*, *114*(D14).

Hantson, S., A. Arneth, S. P. Harrison, D. I. Kelley, I. C. Prentice, S. S. Rabin, S. Archibald, F. Mouillot, S. R. Arnold, P. Artaxo, et al. (2016), The status and challenge of global fire modelling, *Biogeosciences*, *13*(11), 3359–3375.

Horton, D. E., N. S. Diffenbaugh, et al. (2012), Response of air stagnation frequency to anthropogenically enhanced radiative forcing, *Environmental Research Letters*, *7*(4), 044,034.

Horton, D. E., C. B. Skinner, D. Singh, and N. S. Diffenbaugh (2014), Occurrence and persistence of future atmospheric stagnation events, *Nature climate change*, *4*(8), 698–703.

Hou, P., and S. Wu (2016), Long-term changes in extreme air pollution meteorology and the implications for air quality, *Scientific Reports*, *6*, 23,792.

Houghton, J. T., Y. Ding, D. J. Griggs, M. Noguer, P. J. van der Linden, X. Dai, K. Maskell, and C. A. Johnson (2001), Climate change 2001: the scientific basis third assessment report of the intergovernmental panel on climate change.

Huffman, G. J., D. T. Bolvin, E. J. Nelkin, D. B. Wolff, R. F. Adler, G. Gu, Y. Hong, K. P. Bowman, and E. F. Stocker (2007), The TRMM multisatellite precipitation analysis (TMPA): Quasi-global, multiyear, combined-sensor precipitation estimates at fine scales, *Journal of hydrometeorology*, *8*(1), 38–55.

Jacob, D. (1999), *Introduction to atmospheric chemistry*, Princeton University Press.

Jacob, D. J., and D. A. Winner (2009), Effect of climate change on air quality, *Atmospheric environment*, *43*(1), 51–63.

Jacob, D. J., J. A. Logan, R. M. Yevich, G. M. Gardner, C. M. Spivakovsky, S. C. Wofsy, J. W. Munger, S. Sillman, M. J. Prather, M. O. Rodgers, et al. (1993), Simulation of summertime ozone over North America, *Journal of Geophysical Research: Atmospheres*, *98*(D8), 14,797–14,816.

Jacob, D. J., L. W. Horowitz, J. W. Munger, B. G. Heikes, R. R. Dickerson, R. S. Artz, and W. C. Keene (1995), Seasonal transition from NO_x-to hydrocarbon-limited conditions for ozone production over the eastern United States in september, *Journal of Geophysical Research: Atmospheres*, *100*(D5), 9315–9324.

Janhäll, S., K. F. G. Olofson, P. U. Andersson, J. B. C. Pettersson, and M. Hallquist (2006), Evolution of the urban aerosol during winter temperature inversion episodes, *Atmospheric Environment*, *40*(28), 5355–5366.

Jones, A. M., R. M. Harrison, and J. Baker (2010), The wind speed dependence of the concentrations of airborne particulate matter and NO_x, *Atmospheric Environment*, *44*(13), 1682–1690.

Kalnay, E., M. Kanamitsu, R. Kistler, W. Collins, D. Deaven, L. Gandin, M. Iredell, S. Saha, G. White, J. Woollen, et al. (1996), The NCEP/NCAR 40-year reanalysis project, *Bulletin of the American meteorological Society*, *77*(3), 437–471.

Kanamitsu, M., W. Ebisuzaki, J. Woollen, S.-K. Yang, J. J. Hnilo, M. Fiorino, and G. L. Potter (2002), NCEP–DOE AMIP-II Reanalysis (R-2), *Bulletin of the American Meteorological Society*, *83*(11), 1631–1643.

Kinney, P. L. (2008), Climate change, air quality, and human health, *American journal of preventive medicine*, *35*(5), 459–467.

Kloster, S., F. Dentener, J. Feichter, F. Raes, U. Lohmann, E. Roeckner, and I. Fischer-Bruns (2010), A GCM study of future climate response to aerosol pollution reductions, *Climate dynamics*, *34*(7-8), 1177–1194.

Kukkonen, J., M. Pohjola, R. S. Sokhi, L. Luhana, N. Kitwiroon, L. Fragkou, M. Rantamäki, E. Berge, V. Ødegaard, L. H. Slørdal, et al. (2005), Analysis and evaluation of selected local-scale PM_{10} air pollution episodes in four European cities: Helsinki, London, Milan and Oslo, *Atmospheric Environment*, *39*(15), 2759–2773.

Laskin, D. (2006), The great London smog, *Weatherwise*, *59*(6), 42–45.

Lee, I., B. Ambaru, P. Thakkar, E. M. Marcotte, and S. Y. Rhee (2010), Rational association of genes with traits using a genome-scale gene network for Arabidopsis thaliana, *Nature biotechnology*, *28*(2), 149.

Lei, H., D. J. Wuebbles, and X.-Z. Liang (2012), Projected risk of high ozone episodes in 2050, *Atmospheric environment*, *59*, 567–577.

Leibensperger, E. M., L. J. Mickley, and D. J. Jacob (2008), Sensitivity of US air quality to mid-latitude cyclone frequency and implications of 1980–2006 climate change, *Atmospheric Chemistry and Physics*, *8*(23), 7075–7086.

Leung, L. R., and W. I. Gustafson (2005), Potential regional climate change and implications to US air quality, *Geophysical Research Letters*, *32*(16).

Liu, H., D. J. Jacob, I. Bey, and R. M. Yantosca (2001), Constraints from ^{210}Pb and ^{7}Be on wet deposition and transport in a global three-dimensional chemical tracer model driven by assimilated meteorological fields, *Journal of Geophysical Research: Atmospheres*, *106*(D11), 12,109–12,128.

Logan, J. A. (1989), Ozone in rural areas of the United States, *Journal of Geophysical Research: Atmospheres*, *94*(D6), 8511–8532.

Ma, Z., X. Hu, A. M. Sayer, R. Levy, Q. Zhang, Y. Xue, S. Tong, J. Bi, L. Huang, and Y. Liu (2016), Satellite-based spatiotemporal trends in $PM_{2.5}$ concentrations: China, 2004–2013, *Environmental health perspectives*, *124*(2), 184.

Maggioni, V., P. C. Meyers, and M. D. Robinson (2016), A review of merged high-resolution satellite precipitation product accuracy during the tropical rainfall measuring mission (TRMM) era, *Journal of Hydrometeorology*, *17*(4), 1101–1117.

Mahowald, N., S. Albani, S. Engelstaedter, G. Winckler, and M. Goman (2011), Model insight into glacial–interglacial paleodust records, *Quaternary Science Reviews*, *30*(7-8), 832–854.

McKee, D. (1993), *Tropospheric ozone: human health and agricultural impacts*, CRC Press.

McKenzie, D., Z. Gedalof, D. L. Peterson, and P. Mote (2004), Climatic change, wildfire, and conservation, *Conservation biology*, *18*(4), 890–902.

Meehl, G. A., and C. Tebaldi (2004), More intense, more frequent, and longer lasting heat waves in the 21st century, *Science*, *305*(5686), 994–997.

Milionis, A. E., and T. D. Davies (1994), Regression and stochastic models for air pollution II. application of stochastic models to examine the links between ground-level smoke concentrations and temperature inversions, *Atmospheric Environment*, *28*(17), 2811–2822.

Murray, V., and K. L. Ebi (2012), IPCC special report on managing the risks of extreme events and disasters to advance climate change adaptation (SREX).

Ordóñez, C., N. Elguindi, O. Stein, V. Huijnen, J. Flemming, A. Inness, H. Flentje, E. Katragkou, P. Moinat, V.-H. Peuch, et al. (2010), Global model simulations of air pollution during the 2003 European heat wave, *Atmospheric Chemistry and Physics*, *10*(2), 789–815.

Park, R. J., D. J. Jacob, P. I. Palmer, A. D. Clarke, R. J. Weber, M. A. Zondlo, F. L. Eisele, A. R. Bandy, D. C. Thornton, G. W. Sachse, et al. (2005), Export efficiency of black carbon aerosol in continental outflow: Global implications, *Journal of Geophysical Research: Atmospheres*, *110*(D11).

Pearce, J., S. Rathbun, G. Achtemeier, and L. Naeher (2012), Effect of distance,

meteorology, and burn attributes on ground-level particulate matter emissions from prescribed fires, *Atmospheric environment*, *56*, 203–211.

Pfister, G. G., S. Walters, J.-F. Lamarque, J. Fast, M. Barth, J. Wong, J. Done, G. Holland, and C. Bruyère (2014), Projections of future summertime ozone over the US, *Journal of Geophysical Research: Atmospheres*, *119*(9), 5559–5582.

Poumadere, M., C. Mays, S. Le Mer, and R. Blong (2005), The 2003 heat wave in france: dangerous climate change here and now, *Risk analysis*, *25*(6), 1483–1494.

Pye, H. O. T., H. Liao, S. Wu, L. J. Mickley, D. J. Jacob, D. K. Henze, and J. H. Seinfeld (2009), Effect of changes in climate and emissions on future sulfate-nitrate-ammonium aerosol levels in the United States, *Journal of Geophysical Research: Atmospheres*, *114*(D1).

Radke, L. F., P. V. Hobbs, and M. W. Eltgroth (1980), Scavenging of aerosol particles by precipitation, *Journal of Applied Meteorology*, *19*(6), 715–722.

Ramanathan, V., and G. Carmichael (2008), Global and regional climate changes due to black carbon, *Nature Geoscience*, *1*(4), 221–227.

Randerson, J., Y. Chen, G. Werf, B. Rogers, and D. Morton (2012), Global burned area and biomass burning emissions from small fires, *Journal of Geophysical Research: Biogeosciences*, *117*(G4).

Randerson, J. T., G. R. van der Werf, L. Giglio, G. J. Collatz, and P. S. Kasibhatla (2015), Global fire emissions database, version 4,(GFEDv4). ORNL DAAC, Oak Ridge, Tennessee, USA.

Rasmussen, D. J., A. M. Fiore, V. Naik, L. W. Horowitz, S. J. McGinnis, and M. G. Schultz (2012), Surface ozone-temperature relationships in the eastern US: A monthly climatology for evaluating chemistry-climate models, *Atmospheric Environment*, *47*, 142–153.

Rieder, H. E., A. M. Fiore, L. M. Polvani, J.-F. Lamarque, and Y. Fang (2013), Changes in the frequency and return level of high ozone pollution events over the eastern United States following emission controls, *Environmental Research Letters*, *8*(1), 014,012.

Rieder, H. E., A. M. Fiore, L. W. Horowitz, and V. Naik (2015), Projecting policy-relevant metrics for high summertime ozone pollution events over the eastern United States due to climate and emission changes during the 21st century, *Journal of Geophysical Research: Atmospheres*, *120*(2), 784–800.

Rienecker, M. M., M. J. Suarez, R. Gelaro, R. Todling, J. Bacmeister, E. Liu, M. G. Bosilovich, S. D. Schubert, L. Takacs, G.-K. Kim, et al. (2011), MERRA: NASA's modern-era retrospective analysis for research and applications, *Journal of climate*, *24*(14), 3624–3648.

Robertson, K. M., Y. P. Hsieh, and G. C. Bugna (2014), Fire environment effects on particulate matter emission factors in southeastern US pine-grasslands, *Atmospheric environment*, *99*, 104–111.

Robine, J.-M., S. L. K. Cheung, S. Le Roy, H. Van Oyen, C. Griffiths, J.-P. Michel, and F. R. Herrmann (2008), Death toll exceeded 70,000 in Europe during the summer of 2003, *Comptes rendus biologies*, *331*(2), 171–178.

Rosenfeld, D., U. Lohmann, G. B. Raga, C. D. O'Dowd, M. Kulmala, S. Fuzzi, A. Reissell, and M. O. Andreae (2008), Flood or drought: how do aerosols affect precipitation?, *science*, *321*(5894), 1309–1313.

Salzmann, M. (2016), Global warming without global mean precipitation increase?, *Science advances*, *2*(6), e1501,572.

Samset, B. H., G. Myhre, A. Herber, Y. Kondo, S.-M. Li, N. Moteki, M. Koike, N. Oshima, J. P. Schwarz, Y. Balkanski, et al. (2014), Modelled black carbon radiative forcing and atmospheric lifetime in AeroCom Phase II constrained by aircraft observations, *Atmospheric Chemistry and Physics*, *14*(22), 12,465–12,477.

Schnell, R. C., S. J. Oltmans, R. R. Neely, M. S. Endres, J. V. Molenar, and A. B. White (2009), Rapid photochemical production of ozone at high concentrations in a rural site during winter, *Nature Geoscience*, *2*(2), 120.

Schwartz, J., F. Laden, and A. Zanobetti (2002), The concentration-response relation

between pm (2.5) and daily deaths., *Environmental health perspectives*, *110*(10), 1025.

Semenza, J. C., C. H. Rubin, K. H. Falter, J. D. Selanikio, W. D. Flanders, H. L. Howe, and J. L. Wilhelm (1996), Heat-related deaths during the July 1995 heat wave in Chicago, *New England journal of medicine*, *335*(2), 84–90.

Shaposhnikov, D., B. Revich, T. Bellander, G. B. Bedada, M. Bottai, T. Kharkova, E. Kvasha, E. Lezina, T. Lind, E. Semutnikova, et al. (2014), Mortality related to air pollution with the Moscow heat wave and wildfire of 2010, *Epidemiology (Cambridge, Mass.)*, *25*(3), 359.

Shen, L., L. J. Mickley, and E. Gilleland (2016), Impact of increasing heat waves on us ozone episodes in the 2050s: Results from a multimodel analysis using extreme value theory, *Geophysical research letters*, *43*(8), 4017–4025.

Singla, V., A. Satsangi, T. Pachauri, A. Lakhani, and K. M. Kumari (2011), Ozone formation and destruction at a sub-urban site in North Central region of India, *Atmospheric research*, *101*(1-2), 373–385.

Staehelin, J., J. Thudium, R. Buehler, A. Volz-Thomas, and W. Graber (1994), Trends in surface ozone concentrations at Arosa (Switzerland), *Atmospheric Environment*, *28*(1), 75–87.

Stavros, E. N., D. McKenzie, and N. Larkin (2014), The climate–wildfire–air quality system: interactions and feedbacks across spatial and temporal scales, *Wiley Interdisciplinary Reviews: Climate Change*, *5*(6), 719–733.

Steiner, A. L., A. J. Davis, S. Sillman, R. C. Owen, A. M. Michalak, and A. M. Fiore (2010), Observed suppression of ozone formation at extremely high temperatures due to chemical and biophysical feedbacks, *Proceedings of the National Academy of Sciences*, *107*(46), 19,685–19,690.

Stier, P., J. Feichter, S. Kinne, S. Kloster, E. Vignati, J. Wilson, L. Ganzeveld, I. Tegen, M. Werner, Y. Balkanski, et al. (2005), The aerosol-climate model ECHAM5-HAM, *Atmospheric Chemistry and Physics*, *5*(4), 1125–1156.

Tai, A. P., L. J. Mickley, D. J. Jacob, E. M. Leibensperger, L. Zhang, J. A. Fisher, and H. O. T. Pye (2012), Meteorological modes of variability for fine particulate matter ($PM_{2.5}$) air quality in the United States: implications for $PM_{2.5}$ sensitivity to climate change, *Atmospheric Chemistry and Physics*, *12*(6), 3131–3145.

Theoharatos, G., K. Pantavou, A. Mavrakis, A. Spanou, G. Katavoutas, P. Efstathiou, P. Mpekas, and D. Asimakopoulos (2010), Heat waves observed in 2007 in athens, greece: synoptic conditions, bioclimatological assessment, air quality levels and health effects, *Environmental Research*, *110*(2), 152–161.

Thompson, M. L., J. Reynolds, L. H. Cox, P. Guttorp, and P. D. Sampson (2001),

A review of statistical methods for the meteorological adjustment of tropospheric ozone, *Atmospheric environment*, *35*(3), 617–630.

Trenberth, K. E. (2011), Changes in precipitation with climate change, *Climate Research*, *47*(1/2), 123–138.

Trenberth, K. E., and C. J. Guillemot (1998), Evaluation of the atmospheric moisture and hydrological cycle in the ncep/ncar reanalyses, *Climate Dynamics*, *14*(3), 213–231.

Trenberth, K. E., P. D. Jones, P. Ambenje, R. Bojariu, D. Easterling, A. K. Tank, D. Parker, F. Rahimzadeh, J. A. Renwick, M. Rusticucci, B. Soden, and P. Zhai (2007), Observations: surface and atmospheric climate change, in *Climate Change 2007: The Physical Science Basis. Contribution of Working Group I to the Fourth Assessment Report of the Intergovernmental Panel on Climate Change*, edited by S. Solomon, D. Qin, M. Manning, Z. Chen, M. Marquis, K. Averyt, M. Tignor, and H. Miller, chap. 3, pp. 235–336, Cambridge University Press, Cambridge, United Kingdom and New York, NY, USA.

Urbanski, S. (2013), Combustion efficiency and emission factors for wildfire-season fires in mixed conifer forests of the northern Rocky Mountains, US, *Atmospheric chemistry and physics*, *13*(14), 7241–7262.

Van der Werf, G. R., J. T. Randerson, L. Giglio, G. J. Collatz, M. Mu, P. S. Kasibhatla, D. C. Morton, R. S. DeFries, Y. v. Jin, and T. T. van Leeuwen (2010),

Global fire emissions and the contribution of deforestation, savanna, forest, agricultural, and peat fires (1997–2009), *Atmospheric Chemistry and Physics*, *10*(23), 11,707–11,735.

Vautard, R., J. Cattiaux, P. Yiou, J. N. Thepaut, and P. Ciais (2010), Northern Hemisphere atmospheric stilling partly attributed to an increase in surface roughness, nat. geosci., 3, 756–761.

Vingarzan, R. (2004), A review of surface ozone background levels and trends, *Atmospheric Environment*, *38*(21), 3431–3442.

Voulgarakis, A., and R. D. Field (2015), Fire influences on atmospheric composition, air quality and climate, *Current Pollution Reports*, *1*(2), 70–81.

Voulgarakis, A., M. E. Marlier, G. Faluvegi, D. T. Shindell, K. Tsigaridis, and S. Mangeon (2015), Interannual variability of tropospheric trace gases and aerosols: The role of biomass burning emissions, *Journal of Geophysical Research: Atmospheres*, *120*(14), 7157–7173.

Wallace, J., D. Corr, and P. Kanaroglou (2010), Topographic and spatial impacts of temperature inversions on air quality using mobile air pollution surveys, *Science of the total environment*, *408*(21), 5086–5096.

Wang, J. X. L., J. K. Angell, D. J. Baker, and D. L. Evans (1999), Air stagnation climatology for the United States, *NOAA/Air Resource Laboratory ATLAS*, (1).

Wang, Q., D. J. Jacob, J. A. Fisher, J. Mao, E. M. Leibensperger, C. C. Carouge, P. L. Sager, Y. Kondo, J. L. Jimenez, M. J. Cubison, et al. (2011), Sources of carbonaceous aerosols and deposited black carbon in the Arctic in winter-spring: implications for radiative forcing, *Atmospheric Chemistry and Physics*, *11*(23), 12,453–12,473.

Weaver, C. P., E. Cooter, R. Gilliam, A. Gilliland, A. Grambsch, D. Grano, B. Hemming, S. W. Hunt, C. Nolte, D. A. Winner, et al. (2009), A preliminary synthesis of modeled climate change impacts on US regional ozone concentrations, *Bulletin of the American Meteorological Society*, *90*(12), 1843–1863.

Westerling, A. L., H. G. Hidalgo, D. R. Cayan, and T. W. Swetnam (2006), Warming and earlier spring increase western us forest wildfire activity, *science*, *313*(5789), 940–943.

Wu, S., L. J. Mickley, E. M. Leibensperger, D. J. Jacob, D. Rind, and D. G. Streets (2008), Effects of 2000–2050 global change on ozone air quality in the United States, *Journal of Geophysical Research: Atmospheres*, *113*(D6).

Xu, Y., J.-F. Lamarque, and B. M. Sanderson (2018), The importance of aerosol scenarios in projections of future heat extremes, *Climatic Change*, *146*(3-4), 393–406.

Zhang, Y., and Y. Wang (2016), Climate-driven ground-level ozone extreme in the fall

over the southeast United States, *Proceedings of the National Academy of Sciences*, *113*(36), 10,025–10,030.

Appendix A

Copyright permissions and information

This section contains copyright information for chapter 2, which is based on *Hou and Wu* [2016].

A.1 E-mail requesting for reproduction permission

Pei Hou <phou@mtu.edu> Mon, Feb 26, 2018 at 11:03 AM

To: permissions@nature.com

Hello,

I am completing a doctoral dissertation at Michigan Technological University. I would like your permission to reprint my Scientific Reports paper as a chapter in my dissertation. My paper is: Hou, Pei, and Shiliang Wu. "Long-term changes in extreme air pollution meteorology and the implications for air quality." Scientific reports 6 (2016): 23792.

Please tell me if you have any question. Thanks for your help.

Best regards,

Pei

A.2 E-mail granting reproduction permission

Journalpermissions <journalpermissions@springernature.com> Tue, Feb 27, 2018 at 8:59 AM

To: Pei Hou <phou@mtu.edu>

Dear Pei,

Thank you for your email. This work is licensed under a Creative Commons Attribution 4.0 International License, which permits unrestricted use, distribution, and reproduction in any medium, provided you give appropriate credit to the original author(s) and the source, provide a link to the Creative Commons license, and indicate if changes were made. **You are not required to obtain permission to reuse this article.** The images or other third party material in this article are included in the articles Creative Commons license, unless indicated otherwise in the credit line; if the material is not included under the Creative Commons license, users will need to obtain permission from the license holder to reproduce the material. To view a copy of this license, visit http://creativecommons.org/licenses/by/4.0/.

Kind regards,

Oda

Oda Siqveland

Permissions Assistant

SpringerNature

The Campus, 4 Crinan Street, London N1 9XW,

United Kingdom

T +44 (0) 207 014 6851

http://www.nature.com

http://www.springer.com

http://www.palgrave.com